Université de Montréal

A genetic and biochemical analysis of *Lhx3* as a candidate gene responsible for the stubby phenotype in mouse

par

Haidy Tadros
Département de sciences biomédicales
Faculté de médecine

Mémoire présenté à la Faculté des études supérieures
en vue de l' obtention du grade de
Maître ès sciences (M.Sc.)
en Sciences biomédicales

Décembre, 1997

Université de Montréal

Faculté des études supérieures

Ce mémoire intitulé:

«A genetic and biochemical analysis of Lhx3 as a candidate gene responsible for the stubby phenotype in mouse»

présenté par:

Haidy Tadros

a été évalué par un jury composé des personnes suivantes:

Président rapporteur: Dr. Muriel Aubry
Directeur de recherche: Dr. Majambu Mbikay
Membre de jury: Dr. David Silversides

Mémoire accepté le: 23.04.1998

RÉSUMÉ

La souris stubby (*stb*) présente une dépression de la croissance et l'infertilité chez les mâles. Ce phénotype est dû à une mutation récessive d'un seul gène dans la partie proximale de chromosome (Chr) 2. L'infertilité de cette souris n'est pas due à un désordre testiculaire, car la spermatogenèse et la stéroïdogenèse sont normales. Des études de comportement ont démontré que la souris *stb/stb* est incapable de copuler. Elle représenterait donc un modèle d'impuissance sexuelle. L'hyperprolactinémie est une des causes endocrines d'impuissance chez l'homme. Toutefois, nous n'avons pas observé une augmentation consistante d'ARNm de la PRL dans les hypophyses des souris *stb/stb* par rapport aux souris normales. Le locus *stb* se situe sur le Chr 2 à proximité de *Jund-2* (une séquence apparentée à jun), *Dbh* (dopamine beta hydoxylase) et *Notch-1* (homologue de la notch de Drosophile). Nous avons positionné un autre gène appelé *Lhx3* proche de *stb*. La cartographie a été effectuée par analyse de RFLP sur un panel d'ADN du rétro-croisement (backcross) (C57BL/6JEi x SPRET/Ei)F1 x SPRET/Ei. *Lhx3* n'a pu être séparé de *Dbh* et *Notch-1* dans ce panel. Ces deux loci ont été utilisés comme ancres pour positionner *Lhx3* proche de *stb* sur une carte consensus. Chez la souris adulte, l'ARNm de *Lhx3* est principalement exprimé dans l'hypophyse. Il a été détecté aussi dans les cellules qui produisent la prolactine, l'hormone de croissance, et les gonadotrophines. Vu cette expression préférentielle de *Lhx3* dans les cellules hypophysaires et l'importance de ces cellules dans la régulation de la croissance et de la fertilité, *Lhx3* représente le meilleur gène candidat pour la mutation *stb.* Cette hypothèse a été testée par des études comparatives de la structure et de l'expression de la *Lhx3* chez la souris *stb/stb* et la souris normale, ainsi que par analyse des effets d'une mutation éventuelle sur l'expression des hormones hypophysaires. On n'a pas trouvé de différences

de *Lhx3* entre les souris *stb/stb* et les normales. Les études d'expression des hormones hypophysaires chez les souris *stb/stb* ont démontrée une augmentation de 60% de FSH. Des corrélations intéressantes ont été trouvées entre le taux d'expression de PRL versus FSH ainsi que GH versus POMC. Ces corrélations pourraient servir comme marqueurs internes de confirmation du phénotype stb. Une étude globale de l'expression des gènes, par la technique d'étalage différentiel (differential display), effectuée dans l'hypophyse de la souris *stb/stb* et de souris normales a montré des différences d'expression de certains ARNm. L'étude et la caractérisation des messagers exprimés différentiellement chez les souris *stb/stb* pourraient éventuellement permettre l'identification du gène responsable pour la mutation *stb*. On a découvert que les souris *stb/stb* développent des cataractes dans les yeux. Les études histologiques ont démontré des dépôts crystallins dans la couche épithéliale de la cornée. En plus, la rétine de ces souris révèle des altérations dans les couches nerveuses et les ganglions. Ces observations sont nouvelles concernant le phénotype stb. L'ensemble de ces travaux visait à établir si une mutation dans le gène *Lhx3* pourrait causer le phénotype des souris stubby. Les résultats obtenus ne permettent ni d'exclure ni de confirmer le rôle de *Lhx3* dans le phénotype stubby. Nos efforts ont cependant répondu à plusieurs questions majeures et ils ont ouvert plusieurs voies nouvelles de recherche.

SUMMARY

The appearance of heritable phenotypic differences between littermates in a colony of inbred mice has often been the starting point of a search for the gene(s) responsible. An initial step in this task is to determine the chromosomal position of the affected locus. This is usually performed by studying the co-segregation of the phenotype with known phenotypic loci or genes in the progeny of a backcross of F1 mice from interspecific matings. The larger the mapping panel, the stronger the link between the affected locus and the known co-segregating genes. These genes thus become candidate genes for the mutant phenotype. The tissue distribution, the cellular function and the physiological effects of the products of these genes may also be used to support the possibility that they may cause the novel phenotype if mutated. The work presented here uses the above strategies to study the *Lhx3* gene and its product, the Lhx3 protein, as possible causes of the stubby phenotype in mice.

The stubby phenotype is characterized by a depressed body growth and male infertility. It is caused by a single gene mutation on the proximal part of chromosome (Chr) 2. Male infertility in these mice is not caused by a testicular dysfunction, since spermatogenesis and steroidogenesis are normal. Behavioral studies have shown that these mice are unable to copulate and hence may represent a mouse model of impotence. The genetic and/or biochemical reasons for this infertility remain unknown. The stubby (*stb*) locus maps on Chr 2 and has been positionned on consensus maps near several potential candidate genes including *Jund-2* (jun related sequence), *Dbh* (dopamine beta-hydroxylase) and *Notch-1*. We have mapped in the same region an additional gene called *Lhx3,* specifying Lhx3. The Lhx3 protein shares a high degree of homology to the family of LIM homeoproteins. As do most members of this family, Lhx3 was shown to act as a transcriptional factor in promoter activity assays. Lhx3 transcripts are primarily found in the pituitary, starting at embryonic day 11, suggesting that the protein may regulate pituitary organogenesis. It has also been detected in prolactin and growth hormone-producing cells as well as in gonadotropin-producing cells in culture. Considering the preferential expression of *Lhx3* in the pituitary, its presence in pituitary hormone-producing cell lines and the importance of this gland for regulating growth and fertility, *Lhx3* represents a better candidate gene for the *stb* mutation than the other proximal genes. The

first indication of a possible association between *Lhx3* and *stb* came when we positioned it near the *stb* locus. The mapping was performed by *BamH* I RFLP analysis of a DNA panel from a (C57BL/6JEi x SPRET/Ei)F1 x SPRET/Ei backcross. In this panel *Lhx3* did not segregate from *Dbh* and *Notch-1*. These two loci were then used as anchors to position *Lhx3* near *stb* on a larger consensus map. To further verify this linkage, we conducted RFLP analysis of the *Lhx3* gene in *stb* mice but we found no differences relative to their normal littermates. Our sequencing of the cDNA fragments encoding LIM domains again revealed no differences between the two groups. In a preliminary analysis of the level of mRNA for pituitary hormones, we noted a small but significant increase of follicle stimulating hormone (FSH) mRNA in the pituitary of *stb* mice relative to their normal littermates. The transcript levels of other pituitary hormones and Lhx3 were similar between the two groups. Interestingly, an inverse correlation was observed within the two groups for growth hormone (GH) versus pro-opiomelanocortin (POMC) and prolactin (PRL) versus FSH. Finally, a differential display analysis of pituitary mRNA of *stb/stb* versus *stb/+* mice was conducted to search for differences in gene expression. Reproducible differences were observed. These differing mRNAs may represent additional leads toward the identification of the gene for the stubby phenotype.

During the course of our investigation, we discovered a novel phenotype for the *stb/stb* mice. Our colony of stubby mice developped eye problems in the form of cataracts. Histological analysis of the eyes of *stb/stb* mice revealed corneal deposits in the epithelial layer of the cornea, with extensive thickening of the cornea. In the retina, we observe perturbations in the nerve and ganglion layers with vascularisations of the arteries in the choroid. These observations have led to the discovery of a new phenotype for the stubby mouse.

Overall, this work was a limited effort to establish whether a mutation in the *Lhx3* gene may be the cause of the stubby phenotype. The results do not confirm or discount such a link. However, the effort has the merit of having answered some of the most obvious questions associated with the analysis of *Lhx3* gene as a candidate for the stubby phenotype while opening new avenues for investigation.

TABLE OF CONTENTS

LIST OF TABLES

LIST OF FIGURES

LIST OF ABREVIATIONS

°C	degrees Celsius
αGSU	α-glycoprotein subunit
a	nonagouti
A	absorbance
aa	amino acid
ap	apterous
Asp	aspartic acid
bp	base pair
BSA	bovine serum albumin
c	complementary
Chr	chromosome
Ci	curie
cM	centimorgans (10^5 bp)
CNS	central nervous system
CRP	cysteine rich protein
Cys	cysteine
Dbh	dopamine beta hydroxylase
DEPC	diethylpyrocarbonate
e	embryonic day
EDTA	ethylenediaminetetra-acetic acid
FSH	follicle-stimulating hormone
g	genomic
GH	growth hormone
Glu	glutamine
h	hour
HD	homeodomain
His	histidine

Jund2	jun-related sequence
kb	kilobases
LH	luteinizing hormone
min	minute
MOPS	morpholinopropanesulfonic acid
NMR	nuclear magnetic resonance
Notch-1	homolog to Drosophila notch
p	post-partum day
PCR	polymerase chain reaction
PNS	peripheral nervous system
POMC	pro-opiomelanocortin
PRL	prolactin
Pro	proline
RBTN-1	rhombotin 1
RFLP	restriction fragment length polymorphism
rpm	revolutions per minute
RT	reverse transcription
sd	Danforth's short tail
SDS	sodium dodecyl sulfate
sec	second
Ser	serine
stb	stubby
Thr	threonine
TSH	thyroid-stimulating hormone
U	units

ACKNOWLEDGEMENTS

Foremost on this list is my research director, Dr. Majambu Mbikay. I am grateful for his patience, kindness and for making the science exciting. *Rabinah ye kalleek leyah.* I would like to take this chance to thank my friends and colleagues in the lab: Francine Sirois, for her technical advice and correction of the rÈsume; Andrew Chen, for his expertise with the mice; JosÈe Hamelin from Dr. Nabil Seidah's group, for probe fragments and equipment; Fouad Habbouche and Gilles Croissandeau, for sharing in the trials and tribulations of preparing this manuscript; Sylvie ...mond, for her valued secretarial assistance. A special word of thanks goes to my dearest friend and companion James Rochemont, for making every day special with his humour and presence.

My list would not be complete without mentioning my mom and dad, Drs. Sarah and Monib Tadros. These are the two people who have always believed in and encouraged me, and whom I thank God for every morning. Finally and most importantly to my husband, Shoukri Sedrak: my life and love, thank you for your support, countless words of encouragement and help in the preparation of some figures.

This my second greatest work is dedicated to my children, Mary-Elizabeth and James, for they are my real Opus Magnum.

1. INTRODUCTION

1.1. THE STUBBY MOUSE

1.1.1. PHENOTYPE

The stubby (*stb*) mouse was first discovered in a mouse colony at the Jackson Laboratory in 1958. The general appearance of the *stb* mouse is that of a shorter and stockier mouse than normal (Figure 1). This disproportionate dwarfing results in domed heads and short thick tails. Homozygous stubby mice (*stb/stb*) can be identified at about 4 to 5 days of age (Lane and Dickie, 1968). Adults have shorter heads, bodies, and legs than normal, but variation in expression is common. The primary effect of the mutation is a disproportionate shortening in the dimensions of all bones where growth occurs by cartilage proliferation (Miller and Flynn-Miller, 1976). Internally, *stb* mice do not show much reduction in organ weight relative to their normal littermates except for the testes which weigh 57 percent less (Lane and Dickie, 1968).

1.1.2. REPRODUCTION

Homozygous *stb* females are fertile and bring up their litters. In contrast, *stb/stb* males are infertile. Infertility in these mice is not associated with any defect of spermatogenesis and steroidogenesis (Chubb and Nolan, 1985). Histologically, their testes are indistinguishible from those of their normal littermates (*stb/+*). The sperm count and motility are comparable between the two groups and are equally competent at fertilizing eggs *in vitro* (Chubb and Nolan, 1985). Testicular steroidogenesis as assessed by the levels of circulating steroid hormones is also similar (Chubb, 1987). Subsequent natural breeding trials demonstrated that *stb/stb* mice were infertile because they cannot successfully mate. The term infertility groups together those causes which may be responsible for reproductive failure. The causes for infertility in man, are usually grouped into three categories: pre-testicular, testicular and post-testicular (*www.ivf.com/shaban.html*). Pre-testicular causes of infertility involve hypothalamic and pituitary diseases. Testicular causes of infertility include chromosomal abnormalities, defective androgen synthesis or action, trauma and others. Post-testicular causes of infertility include disorders of sperm transport, motility or function and erectile dysfunction. As summarized by Chubb and Henry in Table I, mating parameters indicate that *stb/stb* mice do experience sexual arousal but cannot achieve coitus (Chubb, 1987).

Figure 1

A stubby mouse and its normal littermate.

The *stb* mouse is shown on the left. Note the domed head, shorter body and legs as compared to its normal littermate (on the right). Both are 6 weeks of age. The primary effect of the *stb* mutation is a disproportionate shortening of all bones.

TABLE 1

Comparative analysis of mating parameters between *stb (stb/stb) and normal (+/-) mice* [1] (Chubb, 1987)

	stb/stb	***+/-***
Mount latency (sec)	169.2 ± 28.9 *	90.7 ± 18.1
Intromission latency (sec)	-	168.9 ± 32.4
Mounts without intromission:		
Frequency (mounts/min)	0.92 ± 0.06 *	0.39 ± 0.07
Time per mount (sec)	5.7 ± 0.4	4.8 ± 0.5
Mounts with intromission:		
Frequency (mounts/min)	-	0.71 ± 0.06
Time per mount (sec)	-	27.5 ± 2.1
Total number of thrusts	-	166.3 ± 24.3
Total mounts per min	0.92 ± 0.06	1.1 ± 0.05
Mounts before intromission	-	1.8 ± 0.2
Mounts with intromission before ejaculation	-	7.2 ± 1.3
Head mounts per mouse	1.0 ± 0.3 *	0.1 ± 0.1
Ejaculation latency (sec)	-	585.5 ± 85.6
Ejaculation duration (sec)	-	20.0 ± 0.5
Test period duration (min)	45 ± 0 *	9.8 ± 1.4
Ejaculated sperm (10^{-6})	0	27.3 ± 1.2
Female receptivity score	4 ± 0.1	4 ± 0.2
Number of observations	43	53

[1] Values were derived by determining the mean of each of the 12 mice and calculating the standard error (SE) of the means for all 12 mice tested for each group (mean ± SE).

* Significant difference ($p < 0.05$, Wilcoxon Rank Sum Test).

The cause of the impotence of the *stb* mouse remains to be determined. By analogy with erectile disfunction in human, it could be attributed to vasculogenic, neurogenic, and hormonal causes. Indeed, erection is thought to be initiated by visual, olfactory or tactile stimulation of the central nervous system which is translated, through parasympathetic nerves, in relaxation of the penile muscle, increased blood flow, engorgement of the cavernous spaces of the penis and blood entrapment due to blockage of venous outflow (*www. Sexhealth.org/impotence.htm*). Impotence may also be due to endocrinopathies associated with various disorders such as hypogonadism, diabetes and prolactinoma (Foster et al., 1990; Godeau and Charbonnel, 1993). In most cases of human impotence, however, the causes are psychological rather than physiological.

The study of the *stb* mouse could provide some insights into the physiological forms of male impotence in man and subsequently lead to the development of appropriate approaches for their treatment.

1.1.3. CHROMOSOMAL MAPPING

Genetic analysis indicates that the stubby phenotype is caused by a single gene mutation and that the mutation is recessive (Lane and Dickie, 1968). However, in our hands, mating of heterozygous mutants (*stb/+)* to *stb/stb* females constantly resulted in small litters of 2 to 3 pups; suggesting either that the mutation may be co-dominant or that, in the homozygous state, it may somehow affect the reproductive performance of the female too. The penetrance of the mutation in both genders could eventually be elucidated by appropriate breeding experiments.

The *stb* mutation was initially mapped to mouse chromosome (Chr) 2 by linkage to two other phenotypic mutations, the nonagouti mutation (*a*) and the Danforth's short tail mutation (*Sd*). A three point cross confirmed the linear order of these three loci to be *a-stb-Sd* (Lane and Dickie, 1968).

1.2. CANDIDATE GENES

The mutated gene responsible for the stubby phenotype has not been elucidated yet. On consensus maps of mouse Chr 2, the *stb* mutation is generally positionned near genes that can be considered candidates for the phenotype, because of their tissue distribution and their possible role in development. There are: the gene for a jun-related sequence (*Jund-2*), the gene for dopamine beta-hydroxylase (*Dbh*), the gene for *Notch-1* and the *Lhx3* gene, encoding the Lhx3 protein (Figure 2). In this section, we will briefly describe the relevance of the first three candidate genes. *Lhx3,* which is the subject of our work, will be discussed extensively in section 1.3.

1.2.1. *JUND-2*

Jund-2 has sequence homology with the potent family of jun transcription factors. Members of this family possess leucine zippers that can interact to form homodimers or heterodimers. They are involved in neuronal differentiation, programmed neuronal cell death and neuronal plasticity (Lewin, 1990). The Jund transcriptional factor is a negative regulator of cell growth in various cell lines (Schlingensiepen et al., 1994). Mutations in such transcriptional factors may have profound developmental consequences, including neurological defects.

1.2.2. *DBH*

Dopamine beta-hydroxylase catalyzes the final step in noradrenaline synthesis and is expressed exclusively in noradrenergic and adrenergic cells. The dopamine beta-hydroxylase gene has recently been inactivated in mouse by targeted mutagenesis. *Dbh*-null mice suffer from deficiencies of motor function, learning, and memory. However, these animals show no bone abnormality and their fertility is normal (Thomas and Palmiter, 1997), making *Dbh* an unlikely candidate for the *stb* mutation.

Figure 2

A partial graphic representation of the genetic map of mouse Chr 2

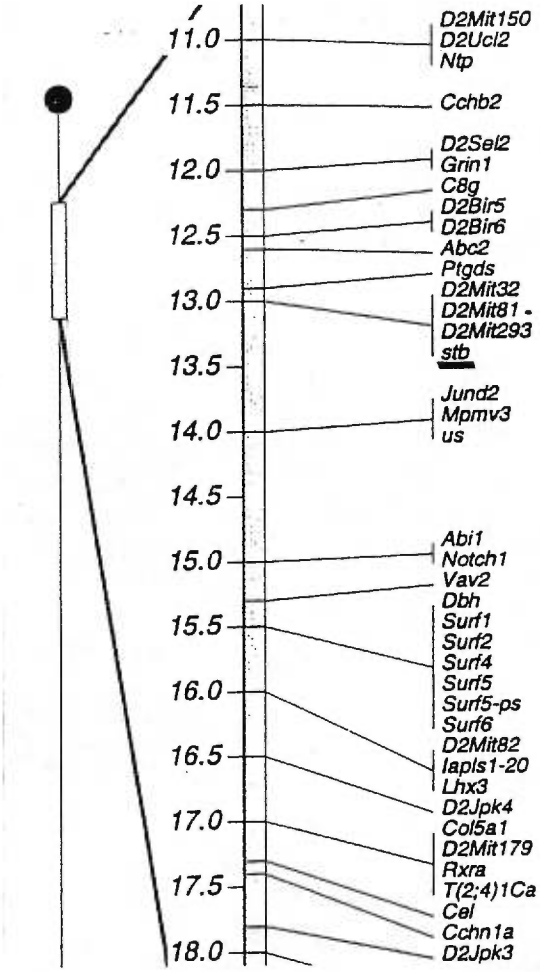

The map is a consensus map derived from several linkage analysis (Lyon and Kirby, 1994). Because of the inherent margin of error in such maps, we consider genes within 2-4 centimorgans (cM; represented by the numbers) from the *stb* locus (underlined) to be candidate genes for the mutation, especially if their pattern of expression, their cellular role and their physiological function can tentatively be associated with the observed phenotype.

1.2.3. *Notch-1*

Notch-1 belongs to a gene family encoding trans-membrane receptors which seem to play important roles in the proliferation and differentiation of the developing central nervous system and peripheral tissues. Their expression begins early in mouse development and corresponding transcripts are found during gastrulation, somitogenesis and early nervous system formation (Williams *et al.*, 1995). This pattern of expression argues for the possibility that a mutation in the *Notch-1* gene could cause serious neurological abnormalities.

1.3. The LIM Family

A family of proteins that carries a cysteine-rich zinc-binding domain called the LIM domain has been studied extensively for their roles in development. These proteins are present in mammals, amphibians, flies, worms and plants and their main function is in developmental regulation. The cysteine-rich motif of the LIM domain was first identified in the protein products of three genes, *lin-11* from *Caenorhabditis elegans* (Freyd et al., 1990), *ISL1* from rat (Karlsson et al., 1990) and *mec-3* from *C. elegans* (Way and Chalfie, 1989). The name LIM is a combination of the first letter of each gene name. LIM proteins form a diverse group which includes transcriptional factors and cytoskeletal proteins.

1.3.1. Classification of Lim proteins

Two main classes of LIM proteins are known (Figure 3). One class contains proteins that have two LIM domains in association with a homeodomain; these are designated LIM-HD proteins. LIM-HD proteins are involved in the control of cell lineage determination and the regulation of differentiation. The second class has no homeodomain, but contains only LIM domains; these are designated LIM-only proteins. Existing subclasses of LIM-only proteins consist of: one to five LIM domains and little else; three to four LIM domains at the C-terminal end; and proteins containing LIM domains with other recognized motifs of varying structure.

Figure 3

LIM family Classification

1. LIM-HD proteins:

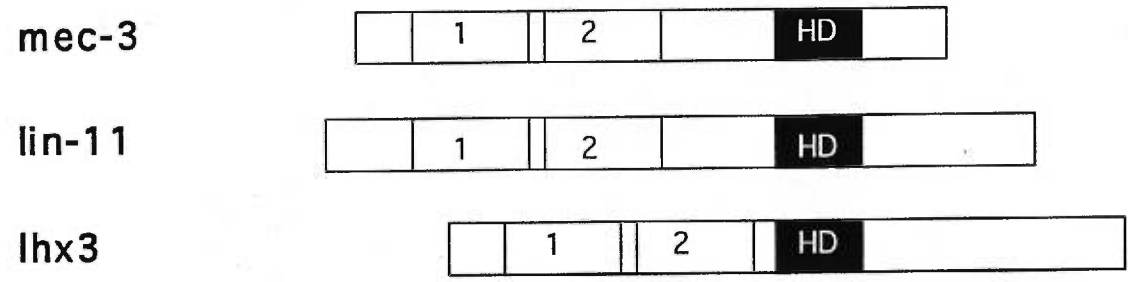

2. LIM-only proteins:

a) 1 to 5 LIM domains

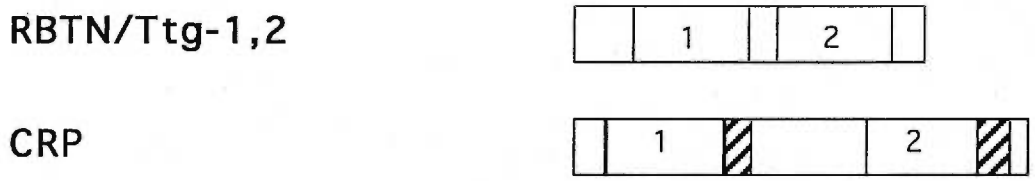

b) 3 to 4 LIM domains at C-terminal end

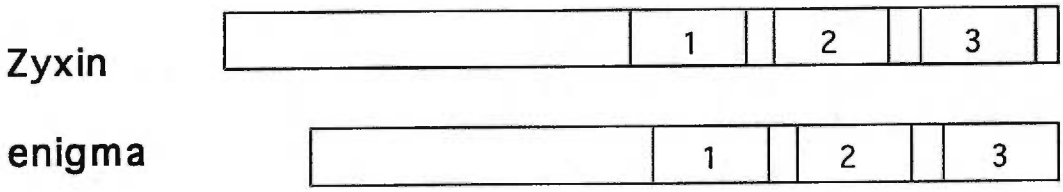

c) LIM domains with other functional regions

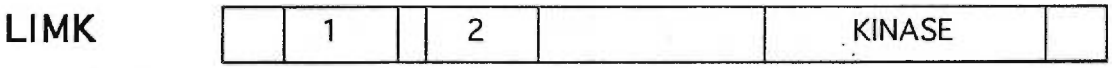

LIM domains are numbered, homeodomains (HD) are shown in blackened boxes, other identified domains are indicated, and a short glycine-rich, conserved region in the CRP is hatched. Figure adapted from Dawid et al., 1995.

LIM-only proteins have been implicated in studies such as; metal binding and zinc-finger proteins, direct protein-protein interactions, regulation of cell proliferation and differentiation, intracellular trafficking, cytoskeletal association and chromosomal translocations.

1.3.1.1. LIM-only proteins

The LIM domain is defined by a conserved pattern of cysteine, histidine or alternate metal-coordinating residues (Figure 4). Each LIM domain coordinates two zinc ions specifically (Archer et al., 1994; Karlsson et al., 1990; Kosa et al., 1994; Michelsen et al., 1993) and thus the LIM domain consists of two specialized zinc fingers connected by a short spacer of two residues (Dawid et al., 1995). It is thought that binding of zinc by these molecules stabilizes the tertiary structure of the LIM domains, generating an interface for protein or nucleic acid interactions (Sanchez-Garcia et al., 1993). Structural analysis by nuclear magnetic resonance (NMR) of the cysteine rich protein (CRP) revealed a protein displaying molecular symmetry, with two LIM domains in tandem, being independent and equivalent with respect to zinc coordination (Michelsen et al., 1993). Furthermore, the C-terminal LIM domain of this molecule showed a second zinc-binding module with strong structural similarity to the zinc fingers in the GATA-1 transcriptional factor and the glucocorticoid receptor (Perez-Alvarado et al., 1994). This similarity with structures known to participate in DNA binding and transcriptional regulation raises the possibility that LIM domains may bind DNA. As yet there is no available evidence that LIM domains possess such a function.

All studies seem to agree with the LIM domain playing an important role in protein-protein interactions. Previous work shows that the LIM-only protein CRP can form homodimers (Feuerstein et al., 1994), and heterodimers with another LIM protein zyxin (Schmeichel and Beckerle, 1994), both activities depending on their LIM domains.

Figure 4

Zinc coordination in the LIM domain

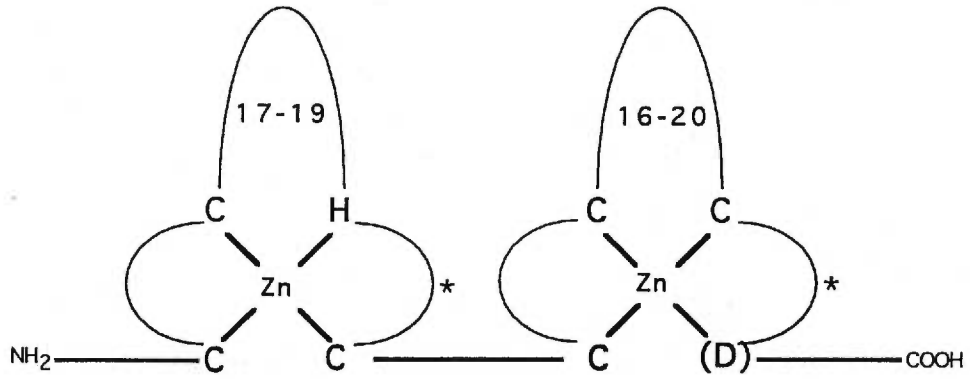

H

C - xx - C - X17-19 - H - xx - C - xx - C xx - C - X16-20 - C - xx - D - x

C

The length of loops ranges from 16-23 amino acids when considering different LIM proteins. Above is a consensus sequence of a LIM domain for proteins in this family (C= cysteine, D= aspartic acid, H= histidine). The asteriks (*) denote that spacing varies from the standard two amino acids in various proteins. Between parantheses is a variable amino acid for different LIM proteins (either D,C or H). Figure adapted from Dawid et al., 1995.

Along with CRP, zyxin interacts directly with the cytoskeletal protein α-actinin (Crawford et al., 1992), implicating both these LIM proteins in the regulation of cytoskeletal function. The LIM-only proteins Rhombotin 1 and 2 (RBTN or Ttg 1,2) were discovered as putative oncogenes because of their activation by chromosomal translocations in T cell acute lymphoblastic leukaemia (Boehm et al., 1991; McGuire et al., 1992; Royer-Pokora et al., 1991). Both these genes have been shown to cause leukaemia and lymphoma in transgenic mice (Fisch et al., 1992). This is a prime example for their involvement in cell proliferation. In addition, the LIM domains of RBTN-1,2 and the basic helix-loop-helix protein Tal1, form a complex with each other in erythroid cells (Valge-Archer et al., 1994). Binding of the C-terminal LIM domains of the novel molecule *enigma* to a region in the insulin receptor known to mediate endocytosis has been shown (Wu and Gill, 1994), implying a function for this particular LIM protein in endocytosis.

1.3.1.2. LIM-HD proteins

The genes belonging to this class contain a common segment of about 180 base pairs (bp) specifying a homeodomain (HD). Proteins encoded by these genes contain two copies of the cysteine-rich LIM domain (as described previously), in association with a HD. These proteins function as transcriptional factors as the HD is a well established DNA-binding domain (Scott et al., 1989). As described above for LIM-only proteins, the LIM domain of LIM-HD proteins are implicated in protein-protein interactions, while the HD binds specific DNA sequences regulating gene transcription. In LIM-HD proteins, the LIM domains seem to function as negative regulatory domains, by inhibiting DNA binding by the HD; such is the case for Mec-3 and Isl-1 proteins (Sanchez-Garcia et al., 1993; Xue et al., 1993). Xue *et al.* (1993) showed that Mec-3 is required for the differentiation of certain *C. elegans* mechanosensory neurons by cooperating with another homeoprotein, Unc-86. In addition, functional studies by German et al.(1992), showed that reporter constructs containing the insulin gene promoter were weakly activated by full-length Imx-1, and more strongly by Imx-1 from which the LIM domains had been removed. Interestingly, much higher stimulation of expression was achieved by cotransfection of the reporter with full-length *Lmx-*

1 and *Pan-1* (a hamster homolog of the helix-loop-helix protein E47) in expression constructs. In *Xenopus* embryos, a functional study of *Xlim-1* in the Spemann organizer also suggests a negative role for the LIM domains (Taira et al., 1994). It was proposed that the wild type Xlim-1 protein is an essentially inactive form in which the LIM domains inhibit the function of the other regions of the protein. Thus, activation of gene transcripts may be achieved by intermolecular interaction of the LIM domains of LIM-HD proteins with a region on enhancer molecules, or by artificially mutating the LIM domains, thereby removing the interference with DNA binding.

The expression patterns of many genes which encode LIM-HD proteins indicate that they play a role in the basic mechanisms of cellular differentiation. A good example is the *Drosophila* gene *apterous* (*ap*), which clearly has multiple functions. *Ap* is expressed in the wing and haltere imaginal discs and is required for wing pattern formation (Cohen et al., 1992). In addition, *ap* is expressed in certain muscle precursor cells in the embryo, and in the absence of *ap* function a subset of abdominal muscles fail to form (Bourgouin et al., 1992). Widespread expression of *ap* in the central nervous system implies that this gene functions in fly development (Bourgouin et al., 1992; Cohen et al., 1992). In *C.elegans* one of the founding genes, *lin-11* encodes a protein that controls certain asymmetric cell divisions during vulval development (Way and Chalfie, 1989). The mouse homolog of *Xlim-1*, *lim-1* is highly conserved and its expression pattern is similar to that of *Xlim-1* (Barnes et al., 1994). Both genes are expressed in the developing kidney and nervous system. As revealed by its expression pattern during mouse embryogenesis and in adult animals, *lim-1* may have a role in early mesoderm formation in the embryo, then later in the kidney and CNS (Barnes et al., 1994).

LIM-HD genes are widely expressed, especially in the nervous system. A few examples of this include: rat *Isl-1* proved to be widely although not ubiquitously expressed in the CNS and PNS (Dawid et al., 1995); the mouse gene *lim-2* is expressed in pituitary development and may be involved in transcriptional regulation of the α subunit of pituitary glycoprotein hormones

(Roberson et al., 1994); extensive work in chickens has shown that while no single LIM gene defines motor neuron columns, a combinatorial expression of four such genes can segregate into columns in the spinal cord and select distinct axonal pathways (Tsuchida et al., 1994); finally, the mouse *lim-3* (*Lhx3*) gene is expressed in the pituitary as well, and is found to be a very early marker concerned with the initial determination of the pituitary (Seidah et al., 1994). This gene which is the focus of our work will be described in greater detail in the following section.

1.3.2. THE *LHX3* GENE AND ITS GENE PRODUCT

The *Lhx3* gene was independently discovered by three groups and given three different names. One group refers to it as factor P-Lim (Bach et al., 1995), another group calls it the *Lhx3* gene (Zhadanov et al., 1995a) and the last group calls it *mLim-3* (Seidah et al., 1994). The International Committee on Mouse Gene Nomenclature has proposed that LIM-HD genes be named *Lhx* and numbered, following the proposals by Scott (1992). For clarity, we shall adopt the *Lhx3* gene name, to distinguish it from the zebrafish genes of this family (*lim-n*); hence, the gene products will be named Lhx3.

1.3.2.1. Structure

The cDNA sequence of Lhx3 is 2,213-bp long and contains an open reading frame of 1,200 bp coding for 400 amino acids (Seidah et al., 1994). Assuming a poly(A) tail of 200-300 bases in length, the total sequence corresponds to an mRNA of 2.4 kb (Figure 5).

Figure 5

The sequence, gene structure and protein organization of Lhx3

A. Nucleotide and amino acid sequence: The 4 major regions of the *Lhx3* gene products are underlined with brackets (LIM-A, LIM-B, HD = homeodomain, PEST). Primer sequences used for PCR-sequencing of the gene are outlined with bold arrows (corresponding to their orientation: S = sense, AS = antisense). The amino acid sequence is given below the nucleotides. (Seidah et al., 1994: accession number L33776 from GenBank).

B. Graphic representation of *Lhx3* gene structure: Exonic sequences are denoted with boxes while the lines represent intronic sequences. Exons (numbered 1-6) coding for LIM-A, LIM-B, HD and PEST regions are represented as vertical lined, hatched, squared and filled boxes, respectively. Note the HD spans 2 exons while the other regions are confined to single exons.

C. Graphic representation of the Lhx3 protein: Organization of the major regions in the Lhx3 protein are presented and given the same drawing fonts as in part B.

A. Nucleotide and amino acid sequence

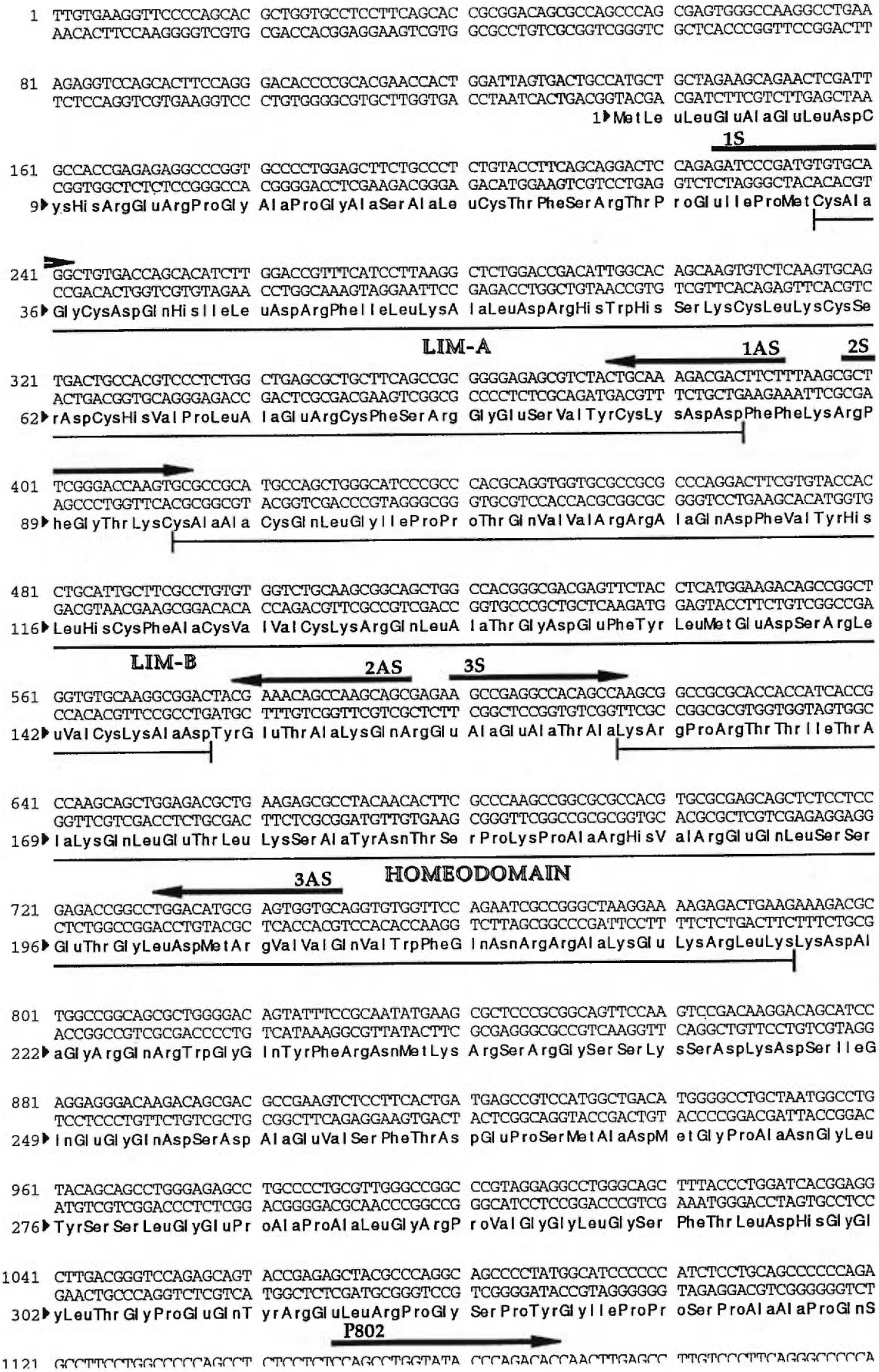

```
     CGGAAGGACCGGGGGTCGGA GAGGAGAGGTCGGACCATAT GGGTCTGTGGTTGAACTCGG AACAGGGAAGTCCCGGGGGT
329▶ erLeuProGlyProGlnPro LeuLeuSerSerLeuValTy rProAspThrAsnLeuSerL euValProSerGlyProPro

1201 GGTGGACCCCCACCCATGAG GGTGCTGGCTGGAAATGGGC CCAGCTCCGACCTGTCCACA GAGAGCAGTTCTGGCTACCC
     CCACCTGGGGGTGGGTACTC CCACGACCGACCTTTACCCG GGTCGAGGCTGGACAGGTGT CTCTCGTCAAGACCGATGGG
356▶ GlyGlyProProProMetAr gValLeuAlaGlyAsnGlyP roSerSerAspLeuSerThr GluSerSerSerGlyTyrPr
                                                                    PEST

1281 AGACTTTCCTGCTAGCCCTG CTTCCTGGCTGGATGAAGTA GACCATGCTCAGTTCTGACC GAGGCCTCTGCTTCCCCTGG
     TCTGAAAGGACGATCGGGAC GAAGGACCGACCTACTTCAT CTGGTACGAGTCAAGACTGG CTCCGGAGACGAAGGGGACC
382▶ oAspPheProAlaSer ProA laSerTrpLeuAspGluVal AspHisAlaGlnPhe
                                  P807
1361 CTCTAACTCAGGGGTCTTGG TGCTGCCTCTGGGTGGATGG CTAGCCCCATCCCATGCTGT CCATTCCAAGGACCTCTGAG
     GAGATTGAGTCCCCAGAACC ACGACGGAGACCCACCTACC GATCGGGGTAGGGTACGACA GGTAAGGTTCCTGGAGACTC

1441 GGAAGGACAGGGTTCCCAAG TGAGAGAATAGGGACTGTCC CACTTCCAGGCTCTCTGGCA GCTCCCTGGGGCTGAGGGAC
     CCTTCCTGTCCCAAGGGTTC ACTCTCTTATCCCTGACAGG GTGAAGGTCCGAGAGACCGT CGAGGGACCCCGACTCCCTG

1521 TCCAAAGTCCTTCCTTGGAC ACAAGGGTGGCCTGCCTGGT GGCTGTCCACAAGCCAGTGA CCATTTCTTGTAAGCATTTC
     AGGTTTCAGGAAGGAACCTG TGTTCCCACCGGACGGACCA CCGACAGGTGTTCGGTCACT GGTAAAGAACATTCGTAAAG

1601 TCTTTCTTTACTGGCCAGTT AACCCTTGCTGCTATTTCCG ACAGGGCAGGAGGCTAGGCC TACCTAATGTCCTGGCAGAA
     AGAAAGAAATGACCGGTCAA TTGGGAACGACGATAAAGGC TGTCCCGTCCTCCGATCCGG ATGGATTACAGGACCGTCTT

1681 AACAACAGTAACGCCTTGCT TCATCGCTTCTGATGGGGCT TGGTAGGAGACTGTGCTTGT GTCCTTCCTGGCCACTGACA
     TTGTTGTCATTGCGGAACGA AGTAGCGAAGACTACCCCGA ACCATCCTCTGACACGAACA CAGGAAGGACCGGTGACTGT

1761 AAACCTGGGAGCACACCTCT CCTCCTTACTGCTGCCAGCT CTCCCTCCCCGGAGTCTCCA GATCATTCTGTTCTGGAATG
     TTTGGACCCTCGTGTGGAGA GGAGGAATGACGACGGTCGA GAGGGAGGGGCCTCAGAGGT CTAGTAAGACAAGACCTTAC

1841 CCGTGTGTTGGGGGAGTAGA GCTTTCTGGAGCCCCTTCTC CAAGGCGTAGCCTCTAAATG CGAGAACAATTCCCCTTCGA
     GGCACACAACCCCCTCATCT CGAAAGACCTCGGGGAAGAG GTTCCGCATCGGAGATTTAC GCTCTTGTTAAGGGGAAGCT

1921 GCACAGCCTCCCTCGGGTGC AAAGCAGAATTGTGCACCGT GAACAGACACCTTTGCCAAA CAGACTGTGGTCCCGAGCAG
     CGTGTCGGAGGGAGCCCACG TTTCGTCTTAACACGTGGCA CTTGTCTGTGGAAACGGTTT GTCTGACACCAGGGCTCGTC

2001 GGTCGGGGGGTGGTTCCACT GGAGGAGGCTGGGCTGGGGG TCCTCCCAACCCAATCTGTC TCAGACACAAAGCTTGACCA
     CCAGCCCCCCACCAAGGTGA CCTCCTCCGACCCGACCCCC AGGAGGGTTGGGTTAGACAG AGTCTGTGTTTCGAACTGGT

2081 CGTGAAAGTTAAGATCATTC CTGAAAACAGGATCTTGGCT ACCTGTTGGTTCTGTAAACA CCCTGTAACTTTTATTTATT
     GCACTTTCAATTCTAGTAAG GACTTTTGTCCTAGAACCGA TGGACAACCAAGACATTTGT GGGACATTGAAAATAAATAA

2161 CCCTGGTGATCCGCTCTTTC CAAGACTTCAATAAATTTGT CAGTTTCAGAGCT
     GGGACCACTAGGCGAGAAAG GTTCTGAAGTTATTTAAACA GTCAAAGTCTCGA
```

B. Graphic representation of *Lhx3* gene structure

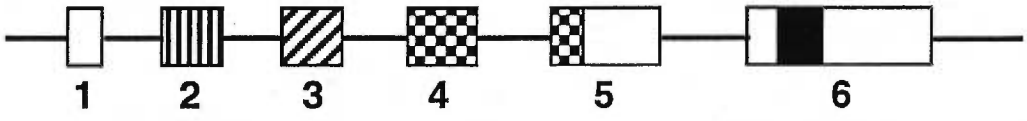

C. Graphic representation of the Lhx3 protein

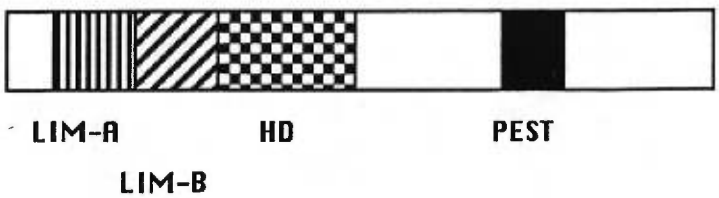

This sequence was found to be closest to *Xenopus Xlim-3*, exhibiting 78% and 66% sequence homology at the protein and nucleotide levels, respectively. The homology is even greater within the two LIM domains and the homeodomain of the Lhx3 protein and that of *Xenopus*, being 81%, 95% and 97%, respectively (Zhadanov et al., 1995b).The linker amino acid sequence between the two LIM domains is identical to that found in *Xenopus*; whereas that between the second LIM domain and the homeodomain is conserved at 91% (Zhadanov et al., 1995b). We shall distinguish the two LIM domains from other members of this family by denoting them as LIM-A and LIM-B. The sequence identity of the LIM-A and LIM-B domains is approximately 57% when compared to their equivalent in other LIM containing proteins (Seidah et al., 1994). However, as reported Seidah et al. (1994), all members of the LIM-HD proteins carry a conserved extra cysteine residue within the LIM-A domain.

The predicted secondary structure of the 59 amino acid homeodomain of the Lhx3 protein is in general agreement with those proposed for other homeoproteins (Scott et al., 1989). Lhx3 differs from Xlim-3 in the homeodomain by only two residues, again arguing that Lhx3 represents the mouse homolog of Xlim-3.

Seidah et al. (1994) reported that as in Xlim-3, the C-terminal segment of the Lhx3 protein is relatively rich in neutral and acidic residues [such as Pro., Glu., Ser., and Thr. (PEST)]. This segment is thought to be important in compensating for the highly basic homeodomain. Although this point has not been studied for Lhx3, this PEST domain is predominantly found in proteins with intracellular half-lives of less than two hours (Rechsteiner, 1989). The presence of such a domain in the Lhx3 protein suggests that this molecule has a short intracellular lifespan.

1.3.2.2. Function and expression

Northern blot analysis of the expression of *Lhx3* in the adult mouse revealed a single transcript of 2.4 kb in the pituitary gland (Zhadanov et al., 1995a); specifically found in the anterior and neurointermediate lobes of the pituitary (Seidah et al., 1994). Lhx3 mRNA was not detected in various brain regions nor

in other organs. This led to the systematic screening of various cell lines including those from rat and mouse pituitary tumours. Transcripts of *Lhx3* were mostly detected in cells of hypophyseal origin, including somatomammotrophs (GH1, GH3 and GH4C1) and gonadotrophs (αT3-1) (Seidah et al., 1994; Zhadanov et al., 1995a). Discrepant results were reported for the corticotrophic mouse cell line AtT-20, in which Seidah's group detected a very low level of *Lhx3* expression whereas Zhadanov's group mentions that expression in this cell line is notably absent.

Developmental expression patterns of *Lhx3,* as visualized by *in situ* hybridization, starts as early as embryonic day (e) 9.5 (Zhadanov et al., 1995a). Experiments with e7.5 and e8.5 embryos revealed no specific signal. By day e9.5 transcription of the *Lhx3* gene was detected in Rathke's pouch and in the closing neural tube. The hypophyseal primordium is mainly represented by Rathke's pouch. In this tissue, the level of hybridization increases significantly particularly between e12 and e14 where maximal expression is observed (Seidah et al., 1994). The ventral epithelium of Rathke's pouch gives rise to the anterior pituitary, called the pars distalis, whereas the dorsal epithelium contributes to the intermediate lobe, called pars intermedia. These two structures are clearly identified by e14 (Rugh, 1991). Embryos at e16.5 showed widespread expression of *Lhx3* in the intermediate and anterior lobes, but not in the posterior lobe (Zhadanov et al., 1995a). Lower levels of expression of *Lhx3* in both the anterior and intermediate lobes of the adult pituitary have been reported by Seidah et al. (1994).

Developmental expression of *Lhx3* in the central nervous system was observed from e9.5 onward by *in situ* hybridization (Zhadanov et al., 1995a). A cross section of e9.5 embryos localizes *Lhx3* to cells in the ventral regions of the neural tube. By e10.5, the zone of *Lhx3* expression extends in an anterior direction to ventral fields of the hindbrain. At e11 the major *Lhx3* expression is detected within the ventral portion of the presumptive pons, medulla and spinal cord (Seidah et al., 1994). Within the spinal cord the intensity of hybridization is maximal within two thin columns along the longitudinal axis, a region populated

by the pre-motor neurons (Seidah et al., 1994). By e13 a maximal expression within the hindbrain, medulla and spinal cord is observed, always as a polarized ventral position. On e18, a period when the spinal cord is structurally and functionally complete, *Lhx3* transcripts can be detected at lower levels in the pons and spinal cord, up to post-partum day (p) 1 (Seidah et al., 1994). Seidah's group shows a repression of *Lhx3* mRNA following this early post-partum period where expression is not detected on p7, p15 and in the adult.

Developmental expression of *Lhx3* within the primordium of the pineal gland was also found starting at approximately e16 and not before (Seidah et al., 1994). As soon as the lobular structures of the pineal gland became distinct on e16, the hybridization signal appeared within a narrow layer of peripheral cells. An increase in the signal was observed by this same group on e18 within the layer of peripheral cells as well as the onset of *Lhx3* expression within the interior of the gland populated by glandular cells. By e20, *Lhx3* expression was observed all over the pineal gland including its peripheral and central divisions, but not in the surrounding tissues (Seidah et al., 1994). This developmental pattern of *Lhx3* expression in the pineal gland only reported by Seidah et al. (1994), will become particularly relevant in view of our findings on the effects of the *stb* mutation on the eyes.

In promoter activity assays, Lhx3 protein was found to act as a transcriptional factor, by stimulating expression of the luciferase reporter gene from the promoter of the gonadotropin α subunit gene (Bach et al., 1995). This is as yet one example of the DNA binding capacity of this LIM homeoprotein. There is also evidence that the Lhx3 protein works in synergy with the transcriptional factor Pit1 to activate prolactin (PRL), thyrotropin-stimulating hormone β subunit (βTSH) and *pit1* genes (Bach et al., 1995). Deletion of the LIM domains of Lhx3 abolishes this synergy, consistent with the involvement of the LIM domains of LIM-HD proteins in the activation of the insulin gene, as reported by German et al. (1992).

The temporal and spatial expression patterns of *Lhx3*, in addition to reporter gene assays suggest that *Lhx3* may play a role in both pituitary

commitment and cellular differentiation events. The generation of disrupted *Lhx3* mice has allowed analysis of the physiological functions of this gene.

1.3.2.3. Inactivation

Targeted gene disruption in mice of the *Lhx3* gene shows that embryos homozygous for the *Lhx3* mutation were either stillborn or died 24 hours after birth (Sheng et al., 1996). The exact cause of death is not known, but it may have resulted from deficits in brain stem function since *Lhx3* is expressed in the precursor cells of the pituitary and during the development of the central nervous system. Although the hindbrain, spinal cord and pineal gland were normal, the *Lhx3* mutant embryos lacked the anterior and intermediate lobes of the pituitary (Sheng et al., 1996). Histological analysis of mutant embryos showed that Rathke's pouch was initially formed in *Lhx3* deficient mice but failed to grow (Sheng et al., 1996). Needless to say this was accompanied by changes in the expression of pituitary specific marker genes. One such gene is the *Rpx* homeobox gene which is expressed very early in pituitary ontogeny in the anterior neural plate and Rathke's pouch (Hermesz et al., 1996). At e10.5 *Rpx* expression was detected in the pouch epithelium of both wild type and *Lhx3* mutant embryos; whereas at e12.5 *Rpx* expression continued in the wild type pituitary but had ceased in the *Lhx3* deficient pouch (Sheng et al., 1996). The loss of *Rpx* expression marks the first detectable alteration in the developmental program of the primordial pituitary cells and establishes the time between e10.5 and e12.5 as a critical period for *Lhx3* gene function in pituitary organogenesis (Sheng et al., 1996). The gene encoding the α-glycoprotein subunit (*αGSU*), is normally the first hormone gene to be activated in the pituitary. The activation of the other peptide hormone genes follows that of the *αGSU* gene and occurs in a specific order during pituitary ontogeny (Simmons et al., 1990). Sheng's group found that in the wild-type mouse, *αGSU* was expressed in the rostral tip of the pituitary at e12.5, and in cells distributed throughout most of the pituitary at e15.5; whereas, *αGSU* expression was undetectable in the *Lhx3* deficient embryos at both these time points. These observations confirm the reporter gene

activation studies done by Bach's group (Bach et al., 1995). Interestingly, *pit-1* transcription was not activated in *Lhx3* mutant embryos (Sheng et al., 1996). Accordingly, the Lhx3 protein not only synergizes with pit-1 in regulating downstream gene expression (Bach et al., 1995), but is also required to activate either directly or indirectly the *pit-1* gene itself (Sheng et al., 1996). Four lineages of the anterior pituitary (thyrotrophs, gonadotrophs, and *pit-1* dependent somatotrophs and lactotrophs) are specifically depleted in *Lhx3* deficient mutants (Sheng et al., 1996), suggesting that *Lhx3* expression is required for the cells of the pituitary primordium to commit to these specific lineages. These observations also suggest that the pathway for gene expression in the pituitary primordium is: *Rpx, Lhx3,* α*GSU* and *pit-1*. Expression of pro-opiomelanocortin (POMC), the ACTH precursor expressed by anterior pituitary corticotrophs is not effected by the mutation in the *Lhx3* gene (Sheng et al., 1996). Thus, the specification of the corticotroph cell lineage occurs in the absence of *Lhx3* gene activity, confirming Zhadanov et al. (1995a) who reported the absence of *Lhx3* expression in the corticotrophic cell line AtT-20.

These results confirm the recessive trait of a *Lhx3* mutation, where heterozygotes are normal. The *Lhx3* deficient embryos provide a genetic model for the study of the early development of the pituitary in mammals, yet they do not implicate the *Lhx3* gene in any known human or mouse diseases.

1.3.2.4. Chromosomal localization

The *Lhx3* gene was localized by *in situ* hybridization in the 2A2-2C1 region of mouse Chr 2 (Seidah et al., 1994). This was confirmed by our work as presented in the appendix, as well as by Zhadanov *et al.* 1995b, using a mouse interspecific backcross DNA mapping panel. *Lhx3* maps on mouse Chr 2 near the *stb* mutation which causes growth and reproductive defects (Lane and Dickie, 1968). As yet, the mutated gene causing the stb phenotype is not known. *Lhx3*, because of its pattern of expression and its cellular function appears to be a probable candidate.

1.4. Research Objectives

To link a given phenotype or disorder to a gene requires both genetic and biochemical analysis of the gene in question. Our working question is: Could the LIM-HD gene *Lhx3* be responsible for the stubby phenotype in mice?

Considering that *Lhx3*: 1) is predominantly found very early in the pituitary primordium, the CNS and the pineal gland; 2) is required for normal pituitary organogenesis and cell lineage differentiation; 3) has the ability to transactivate pituitary genes; it may play a role in regulating growth and reproduction. The stubby phenotype represents the effects of a single gene mutation, yielding disproportionate dwarfing, an unexplained reproductive dysfunction, and the formation of cataracts (a novel observation found during our studies). The complexity of this phenotype most probably involves many hormones and peptides, perhaps directly or indirectly under the influence of one dysfunctional gene. Finally, the chromosomal mapping of the *Lhx3* locus in close proximity to the phenotypic *stb* locus has led us to study this gene as a potential candidate.

Our investigation combines a genetic and a molecular biological approach. A restriction fragment length polymorphism (RFLP) of the *Lhx3* gene between two distant mouse strains was used to determine its allele distribution and segregation relative to other known loci on Chr. 2. The biochemistry focused on the pituitary gland of *stb* mice and their normal littermates. We tried to assess whether there are any differences in the levels of expression of major pituitary hormones, and whether or not these differences can be attributable to Lhx3. Sequencing by polymerase chain reaction (PCR) and RFLP analysis was used to search for any mutations in the major domains of the *Lhx3* gene in *stb* mice. Finally, the novel technique of differential display was employed to highlight those genes that are differentially expressed in the pituitary of *stb* versus normal mice. This last procedure has revealed novel expressed genes that may play important roles in the expression of the stubby phenotype.

2. MATERIALS AND METHODS

2.1. CHEMICAL PRODUCTS

Ammonium acetate was obtained from Biopharm chemicals (Laval, Quebec). EDTA, Tris-base, NaOH, NaCl, Na_3PO_4, Na_2HPO4, and xylene cyanol FF were purchased from BDH (Toronto, Ontario). Acetic acid, HCl, sodium dodecyl sulfate (SDS), morpholino-phenyl sulfate (MOPS), 37% formaldehyde, ethidium bromide, sodium citrate, isoamyl alcohol, isopropyl alcohol, and ethanol were obtained from Fisher Scientific (Nepean, Ontario). Diethypyrocarbonate (DEPC) was purchased from Aldrich Chemical Company (Milwaukee, WI). Bromocresol green, and bovine serum albumin (BSA) came from Sigma (St.Louis, Mo). Sucrose came from Schwarz/Mann Biotech (Clevland, Ohio). TRIzol reagent (Total RNA Isolation Reagent), nucleotide triphosphates, RNAguard, formamide, Proteinase K, phenol, chloroform restriction and modification enzymes were purchased from Gibco BRL Life Technologies (Burlington, Ontario). Agarose IV was obtained from Amresco (Solon, Ohio). Glutaraldehyde came from J. B. EM Services (Pointe-Claire, Quebec). Paraformaldehyde was purchased from Anachemia (Montreal, Quebec) and the cacodylate acid sodium salt was obtained from J. T. Baker Chemical Co. (Phillipsburg, N. J.).

2.2. MICE AND MOUSE TISSUES

Homozygous stubby (*stb/stb*) mice and their normal littermates (heterozygous *stb/+*) were obtained from The Jackson Laboratory (Bar Harbor, ME) and bred in our animal facility. The *stb/stb* genotype determination was based on the manifestation of the stubby phenotype. As shown in Figure 1, a stubby mouse is clearly distinguishable from its normal littermate. All mouse tissues (pituitary and eyes) were surgically removed and either immediately processed for experiments or frozen in dry ice upon removal and stored at -80 8C, for later use. Four-mm tail ends were cut from *stb/stb* and *stb/+* mice for genomic DNA (gDNA) extraction.

2.3. LINKAGE ANALYSIS PANEL

A mouse interspecific backcross DNA panel established at The Jackson Laboratory was used to determine the genetic linkage of *Lhx3* to other loci (its haplotype) and hence its chromosomal localization. This panel was derived from 94 N2 animals from the backcross (C57BL/6JEi x SPRET/Ei) F1 x SPRET/Ei. Membranes carrying *BamH* I-digested DNA of each of the 94 animals from the backcross panel were analyzed by Southern blot (as outlined in 2.7) to determine the *Lhx3* allele distribution and its segregation relative to other loci.

2.4. EYE HISTOLOGY

Both eyes were removed and directly placed in Telly's fixative (2% glutaraldehyde, 1% paraformaldehyde, 0.1 M cacodylate acid sodium salt pH 7.4). Samples were sent to a pathologist at The Jackson Laboratory, where sections were cut and studied. Their findings are reported below.

2.5. GENOMIC DNA PURIFICATION

Typically, 4-mm mouse tail ends were cut and digested in 500 µl of lysis buffer (50 mM Tris-HCl pH 8.0, 100 mM EDTA, 0.125% SDS with 1 mg/ml Proteinase K) in a 6 ml Serum Sample Tube (SST; Becton Dickinson Vacutainer Systems, Franklin Lakes, N.J.) at 55 °C for 16 hours (h). SST tubes are commonly used for purification of serum from blood samples. For our purpose, they permited single-tube phenol extractions of the digested tails. Once the extractions are spun, the organic phases fall below the agar plug, leaving a purified aqueous phase above. Thus, after Proteinase K digestion, the samples were extracted with an equal volume of a phenol-chloroform-isoamyl alcohol solution (at a ratio of 25:24:1, respectively), mixed by inversion then centrifuged for 10 minutes (min) at 2000 x g. This extraction was repeated in the same tube, then a final extraction was performed with an equal volume of chloroform. The aqueous phase was transferred to an Eppendorf tube which contained 25 µl of 3 M sodium acetate pH 6.0, to which 600 µl of cold (-20°C) isopropanol was added for DNA

precipitation. The sample tubes were centrifuged for 10 min at 14,000 revolutions per minute (rpm) at room temperature. The DNA pellet was rinsed with 75% ethanol, centrifuged again for 5 min, air dried for 10 min and finally dissolved in 200 μl of water. DNA concentration in each sample was determined by spectrophotometry at 260 nm.

2.6. PITUITARY mRNA PREPARATION

Messenger RNA was extracted from pituitaries by the TRIzol Reagent. This reagent is a mono-phasic solution of phenol and guanidine isothiocyanate. Organs were placed directly in 1 ml of TRIzol and homogenized using a 1-cc syringe and 22- gauge needles, by forcing the organs in and out of the syringe several times. The homogenized samples were incubated at room temperature for 5 min to permit complete dissociation of nucleoprotein complexes. Chloroform, 0.2 ml, was then added to the homogenate. Sample tubes were capped, shaken vigorously by hand for 15 seconds (sec), and then incubated at room temperature for 3 min. They were centrifuged at 12,000 x g for 15 min at 4 8C. The upper aqueous phase was transferred to a fresh tube; 0.5 ml of isopropyl alcohol were added to it; the samples were incubated at room temperature for 10 min and then centrifuged at 12,000 x g for 10 min at 4 8C. The supernatant was removed and the RNA pellet was overlaid with 1 ml of 75% ethanol. After mixing and centrifugation at 7,500 x g for 5 min at 4 8C, the ethanol was removed; the RNA pellet was air-dried for 5 min and then dissolved in 15 μl of water. RNA concentrations were determined by spectrophotometry at 260 nm.

2.7. SOUTHERN BLOT ANALYSIS

Genomic DNA was digested with different restriction enzymes. A typical reaction consisted of 20 μg of gDNA with BSA to a final concentration of 100 μg/ml, the appropriate 1X buffer for the enzyme, 100 units (U) of enzyme and water to a final volume of 100 μl. The reaction mixtures were incubated for 16 h at the temperature recommanded by the enzyme manufacturer. The reactions were

then stopped with EDTA to a final concentration of 25 μM and the digested DNA was precipitated by adding half the volume of 7.5 M ammonium acetate and two volumes of 95% ethanol. The sample tubes were placed on dry ice for 10 min, then centrifuged at 14,000 rpm for 15 min at 4 °C. The supernatant was discarded; the DNA pellet was overlaid with 75% ethanol, centrifuged once again for 5 min, air-dried and dissolved in 20 μl of water.

The digested DNA was loaded on a 0.6% agarose gel in TAE (40 mM Tris-acetate, 1 mM EDTA, pH 7.6) buffer and separated by electrophoresis. Upon completion of migration, the gel was treated with 0.25 M HCl for 15 min (for *in situ* partial acid depurination and later alkaline hydrolysis of DNA to facilitate transfer of the higher molecular weight DNA) and then neutralized in the transfer solution (0.4 M NaOH) for 30 min. In the meantime, a nylon membrane (GeneScreen Plus, NEN Life Sciences; Boston, MA) cut to the size of the agarose gel, was primed by soaking it in the transfer solution for 10 min. The digested DNA was then left to transfer to the nylon membrane by capillarity for 3 h. The gel was discarded and the membrane was prehybridized in a 0.5 M Na-PO_4 pH 6.6 and 7% SDS buffer at 65 8C for a minimum of 15 min in a rotating hybridization oven.

The probe was a radiolabelled 1.2-kb fragment of the mouse *Lhx3* cDNA (Seidah et al., 1994). In a typical labeling reaction, 100 ng of the cDNA fragment were mixed with 0.125 U (A260 = 0.1 U/μl) of random hexamers in a final volume of 5 μl in an Eppendorf tube. The mixture was boiled for 5 min, then quenched on ice. The tube was briefly centrifuged to collect the solution to the bottom. Then were successively added, 10 μl of 2.5 X random-priming buffer (0.5 M HEPES pH 6.6, 0.125 M Tris-HCl pH 7.8, 12.4 mM $MgCl_2$, 12 mM beta-mercaptoethanol, 50 μM each of TTP, dGTP and dATP), 100 μCuries (Ci) of α-^{32}P-dCTP (Mandel Scientific Company, Lachine, Quebec; specific activity: 3 KCi/mmol), 6 U of the Klenow fragment of DNA polymerase I and water to a final volume of 25 μl. The reaction mixture was incubated for 4 h at room temperature. The volume was brought to 70 μl with 1X STE (20 mM Tris-HCl pH 7.5, 100 mM NaCl, 10 mM EDTA) then passed through a NucTrap column (Stratagene, La Jolla, CA)

equilibrated with this same buffer. This gel filtration column separates unincorporated nucleotides from radiolabeled DNA or RNA probes. The flow-through was kept, along with the final rinse of 70 µl of 1X STE. Altogether, the purified probe came out in approximately 125 µl in 1X STE. It was denatured, by boiling, for 5 min and added to the prehybridization buffer already on the membrane. Hybridizations were performed at 65 8C for 16 h in a rotating hybridization oven. Membranes were washed 3X for 20 min in 1.5 mM sodium citrate, 15 mM NaCl (0.1 X SSC)-0.1% SDS at 65 °C and autoradiographed on XAR-5 x-ray film (from InterScience, Markham, Ontario).

2.8. NORTHERN BLOT ANALYSIS

Two µg of total RNA were electrophoresed on a 1% agarose gel, transferred to a nylon membrane and probed with a radiolabeled complementary RNA (cRNA) probe produced from mlim3, rPRL, rGH and rPOMC (m= mouse, r= rat) linearized cDNA. Typically, 0.5 g of agarose were dissolved in the microwave with 36 ml of diethypyrocarbonate (DEPC)-treated water. Once dissolved, 5.0 ml of a 10X electrophoresis buffer [0.5 M morpholino-phenyl sulfate (MOPS)-10 mM EDTA, pH 7] was added and the mixture was left to cool down to 60 °C, after which 9.0 ml of 37% formaldehyde was added and the agarose mixture was poured into the gel mold and left to polymerize for 30 min. The RNA was denatured by taking 2 µg in 3.2 µl of 1X MOPS-1 mM EDTA adding 1.8 µl 37% formaldehyde, 5.0 µl formamide and heating the samples at 70 °C for 5 min. Prior to loading 3.0 µl of a heavy dye (H.D.) - ethidium bromide solution [2.0 µl H.D. = 1X MOPS-1 mM EDTA, 0.5% xylene cyanol, 0.5% bromocresol green, 40% sucrose, 180 µl/ml 37% formaldehyde, 50% formamide + 1.0 µl 1.0 mg/ml ethidium bromide] was added. The samples were then loaded onto the gel and electrophoresed at 70 volts for 2 h. After migration the gel was rinsed 4 times for 5 min in DEPC-treated water to remove the formaldehyde and soaked twice for 30 min in the transfer buffer which was 20X SSC. The samples were transferred to a Nytran nylon membrane (Xymotech Biosystems, Mount-Royal, Quebec) by capillarity in 20X SSC buffer for approximately 15 h. After transfer the samples

were fixed to the membrane by baking it at 65 °C for 1 h and then exposing to a (long wavelength = 300-400 microns) U.V. light source at a height of 10 cm for 45 sec. The membranes were stored at room temperature in a sealed plastic bag if not used immediately; otherwise they were prehybridized in a 5% SDS, 400 mM Na-PO_4, 1 mM EDTA pH 7.6, 1 mg/ml BSA and 50% formamide buffer for a minimum of 1 h at 65 °C in a rotating hybridization oven.

The radiolabelled cRNA probes were transcribed from cDNAs in restriction enzyme-linearized plasmids. Plasmids carrying the cDNA for mlim3, rPRL, rPOMC, rGH were linearized with *Xho* I, *BamH* I, *EcoR* I and *Xba* I, respectively. The transcription enzyme used was T7 RNA polymerase for mlim3, rPRL and rPOMC constructs, and SP6 RNA polymerase for the rGH construct. All the constructs were made in our laboratory.

Typically, 150 μCi of α-^{32}P-UTP (Mandel, Lachine, Quebec; specific activity: 3KCi/mmol) were lyophilized and reconstituted in 2 μl of DEPC-treated water; then were added in succession, at room temperature, 1 μl of 10X RNA transcription buffer (400 mM Tris-HCl pH 7.4, 60 mM $MgCl_2$, 100 mM DTT, 40 mM spermidine), 1 μl of 100 mM DTT, 1 μl of 21.1 U/ml RNAguard, 1 μl of 5 mM ATP, 1 μl of 5 mM GTP, 1 μl of 5 mM CTP, 1 μl (500 ng) of linearized DNA construct and 1 μl RNA polymerase (100 U) to bring the final volume to 10 μl. The reaction was incubated at 37 °C for 2 h, then 1 μl of DNAse I (1 U) was added to the reaction mixture and the incubation at 37 °C was resumed for an additional 15 min. The reaction volume was diluted to 70 μl with 1X STE buffer and the probes were purified by gel fitration on NucTrap columns. Probes were then heated at 80 °C for 5 min to insure complete denaturation, and then added to the prehybridization mixture. Hybridizations were carried out for 16 h at 65 °C in a rotating hybridization oven. The membranes were then washed at least twice for 1 h in 0.1X SSC-0.1% SDS at 65 °C and either autoradiographed on XAR-5 x-ray film or exposed in a phosphorimaging plate (Molecular Dynamics, La Jolla, CA).

The phosphorimaging scan of the membranes yielded the intensity of each band

as a pixel value, thus enabling comparative statistical analysis of the relative numbers.

2.9. PCR SEQUENCING OF *LHX3* EXONS

Lhx3 exons were amplified with specific oligonucleotides from gDNA of *stb/stb* and *stb/+* mice, then the DNA products were sequenced using the AmpliTaq Cycle Sequencing Kit following the protocol provided by the manufacturer (Perkin-Elmer, Foster City, CA). A typical PCR reaction mix consisted of: 100 ng gDNA from *stb* and normal mice as template in a 0.5 ml PCR sample tube; 1 μM specific sense and antisense oligonucleotides for each domain to be amplified (Figure 5); 1X PCR buffer (10 mM Tris-HCl pH 8.4, 50 mM KCl, 1.5 mM $MgCl_2$, and 0.01% gelatin); 0.4 mM each dATP, dCTP, dTTP and dGTP; 2.5 mM $MgCl_2$ and 0.5 U of AmpliTaq DNA polymerase. The thermocycler was programmed to begin with a template melting cycle, for at least 1 min at 94 °C, then 35 cycles of melting at 94 °C for 1 min, annealing at 52-58 °C for 1 min, and extending at 72 °C for 1 min. The PCR products were separated by gel electrophoresis, the DNA bands of interest were excised from the gel and extracted by the Geneclean technique of purification (Bio 101 Inc., La Jolla, CA). The technique consists of dissolving the agarose with 6 M NaI then using glassmilk as an affinity carrier for DNA extraction. The DNA binds to the glassmilk at room temperature; it is rinsed several times with a wash solution [a dilution of a NaCl/ethanol/water (NEW) concentrate provided in the kit, with ethanol and water to a final concentration of 48% ethanol] to remove any impurities. The DNA is then eluted in water at 50 °C. The percentage of recovery of bound DNA is approximately 95%.

Sequencing of DNA bands essentially consisted of first radiolabelling the oligonucleotides that were used for amplification with γ-^{32}P-ATP in a kinase reaction mixture. This reaction was carried out with 1.5 μM primer, 50 μCi γ-^{32}P-ATP, 70 mM Tris-HCl pH 7.6 -10 mM $MgCl_2$ (1X kinase buffer), and 30 U of T4 polynucleotide kinase in a 10.8 μl reaction volume. Sample tubes were incubated for 10 min at 37 °C and then 5 min at 90 °C. For each sample, 2 μl of each of the

G, A, T, and C termination mixes with 7-deaza-dGTP were dispensed into 0.5 ml PCR sample tubes, one tube per termination mix, and placed on ice. A reaction mixture was set up for each sample to be sequenced in a 30 μl volume. The components consisted of 1.6 pmoles of ^{32}P- end labelled primer, 1X cycling mix (0.5 U/μl AmpliTaq DNA polymerase, 50 mM Tris-HCl pH 8.8, 50 mM KCl, 2.5 mM $MgCl_2$), and 100 fmoles DNA template. Six μl of this reaction mix were dispensed into each of the four tubes containing the termination mix. Each termination reaction mix was overlayed with 20 μl of mineral oil. Sample tubes were then placed in the DNA thermal cycler (Perkin Elmer, Model 380A, Foster City, CA) which was programmed with 1 cycle at 95 °C for 2 min; 25 cycles at 95 °C for 1 min, 52-58 °C for 1 min, and 72 °C for 1 min; one cycle at 4 °C for a maximum of 45 min, during which time 4 μl of stop solution (95% formamide, 20 mM EDTA, 0.05% bromophenol blue, 0.02% xylene cyanol FF) was added to each tube. The samples were subsequently analysed by first denaturing them at 95 °C for 3 min, chilling them on ice, then loading 2.5 μl of each sample on a 6% sequencing gel (refer to section 2.11). Upon completion, the gel was exposed to an x-ray film.

2.10. DIFFERENTIAL DISPLAY

The RNA used for this protocol was prepared as outlined in section 2.6. The differential display technique was the one provided with the RNAmap kit from GenHunter Corporation (Nashville, TN). Essentially, four reverse transcription reactions for each RNA sample was set up in 0.5 ml PCR tubes, each containing: 1 μM of one of the four $T_{12}MN$ (N = G, A, T or C); 1X Reverse Transcription (RT) buffer (25 mM Tris-HCl pH 8.3, 37.6 mM KCl, 1.5 mM $MgCl_2$ and 5 mM DTT); 20 μM dNTP; 200 ng total RNA in a final volume of 20 μl. The sample tubes were placed in the thermocycler programmed to 65 °C for 5 min, 37 °C for 60 min, 95 °C for 5 min followed by chilling at 4 °C. After 10 min at 37 °C, 1 μl (200 U) of MMLV reverse transcriptase was added to each tube. At the end of the reverse transcription, the tubes were spun briefly and set on ice. The PCR reaction was

set up at room temperature to a final volume of 20 μl for each primer set combination. The reaction contained: 2 μl of the RT-mix as outlined above; 0.2 μM Arbitrary Primer (AP) sets; 1 μM $T_{12}MN$ (the same $T_{12}MN$ used in the RT-mix); 2 μM dNTP; 1X PCR buffer; 1 μl of 1200 Ci/mmole α-^{35}S-dATP (from Mandel, Lachine, Quebec); and finally, 1 U AmpliTaq DNA polymerase (from Perkin-Elmer, Foster City, CA). Sample tubes were mixed well, overlayed with 25 μl mineral oil and placed in the thermocycler which was programmed for 40 cycles as 94 °C for 30 sec, 40 °C for 2 min, 72 °C for 30 sec. This was followed by 1 extending cycle at 72 °C for 5 min then storing the samples at 4 °C before loading on a 6% denaturing polyacrylamide gel. Immediately before loading the gel, 3.5 μl of each sample were mixed with 2 μl of loading dye (95% formamide, 10 mM EDTA pH 8.0, 0.09% xylene cyanol FF, and 0.09% bromophenol blue) and incubated at 80 °C for 2 min. The gel was electrophoresed for about 3.5 h at 60 watts constant power until the xylene dye reached the bottom. The gel was then blotted on a piece of 3M paper, covered with plastic wrap and dried under vacuum on a gel dryer at 80 °C for 1 h. The dried gel was exposed to x-ray film for analysis.

2.11. Standard Laboratory Protocols

Standard molecular biology protocols, such as those regarding the preparation of agarose and sequencing gels, and the preparation of stock solutions, have not been detailed in the section. They were performed as described in *Current Protocols in Molecular Biology* 1995 edition by (Ausubel et al., 1995).

3. RESULTS

3.1 EYE CATARACT: A NEWLY DISCOVERED SYMPTOM OF THE STB PHENOTYPE

The breeding of *stb* mice in our colony had led us to the observation that along with the stubby phenotype, these mice were developing eye problems (sometimes in one eye and sometimes in both). The eye would develop cataracts until the mice would eventually go blind. This eye phenotype has never been reported for the *stb* mutation. In collaboration with Dr. Smith and E.M. Simpson of The Jackson Laboratory, we performed a comparative histology of *stb/stb* and normal heterozygous *stb/+* mice. Four mutants and four normal littermates were examined. Eyes were collected before they developped any visible cataracts. Abnormalities in the form of vascularisation and corneal deposits (Figure 6) were observed in 3/4 *stb/stb* mice and in 0/4 *stb/+* mice. Vascularisations of the arteries found in the choroid of *stb/stb* mice are presented in Figure 6A, indicating an abnormality of the blood supply to the eyes of these mice and perhaps a cause for disorder. Also shown on the same picture is a perturbation of the nerve fiber and ganglion cell layers of the retina of *stb/stb* mice not seen in their normal littermates. Whereas these layers are even and smoothly distributed in normal mice eyes, eyes from *stb/stb* mice show an uneven distribution of the nerve fibers and gross morphological changes to the ganglion cells. Figure 6B shows a thickening of the corneal epithelium of the cornea of *stb/stb* mice which is not present in their normal littermates. This thickening is due to abnormal deposits (referred to as corneal deposits) which eventually interfere with rays of light entering the cornea, leading to blindness. The cornea owes its transparency to the presence of a regular lattice structure of collagen fibers. Anything which affects this regularity results in the loss of the transparency which is essential for good corneal function. The pathology observed in *stb/stb* mice resembles human congenital hereditary corneal dystrophy, a very rare disorder of endocrine origin afflicting the ground substance of the eye and associated with collagen anomalies (Maumenee, 1960). This new discovery makes the *stb* mouse an

additional animal model of eye disorders.

3.2. LINKAGE MAPPING OF THE *LHX3* GENE

A prerequisite for linkage mapping is the determination of a polymorphism between two distant strains of mice. First generation heterozygotes (F1) are then backcrossed to one of the parental strains where recombination and allele segregation takes place. The pattern of allele segregation (of each offspring from this backcross) is used to match with known genetic markers for chromosomal localization. The first analysis of backcross data is directed at determining the existence of linkage to the locus of interest. This is done by comparing the pattern of allele segregation of the new locus with the patterns of allele segregation from known marker loci. Essentially, the frequency of recombination between the new locus and each marker locus is calculated, one at a time (Silver, 1995). This task is performed easily by entering the accumulated allele segregation data into an electronic file that is then analyzed by a special computer program. For linkage mapping of the *Lhx3* gene, RFLPs between *Mus musculus* C57BL/6JEi and *M. spretus* SPRET/Ei mouse strains were sought by Southern blot analysis of their gDNA digested with five restriction enzymes (*BamH* I, *Pst* I, *Kpn* I, *Sal* I and *Xho* I), using a 1.2 kb fragment of the mouse *Lhx3* gene as probe (J. C. Barale and N. G. Seidah, unpublished). A *BamH* I RFLP was selected for our mapping. This restriction enzyme produced a fragment of 14.5 kb in C57BL/6JEi and of 25 kb in SPRET/Ei (Figure 7).

Figure 6

Eye abnormalities found in the stb mouse as compared to its normal littermate

A. The Retina and Choroid

stb/stb ***stb/+***

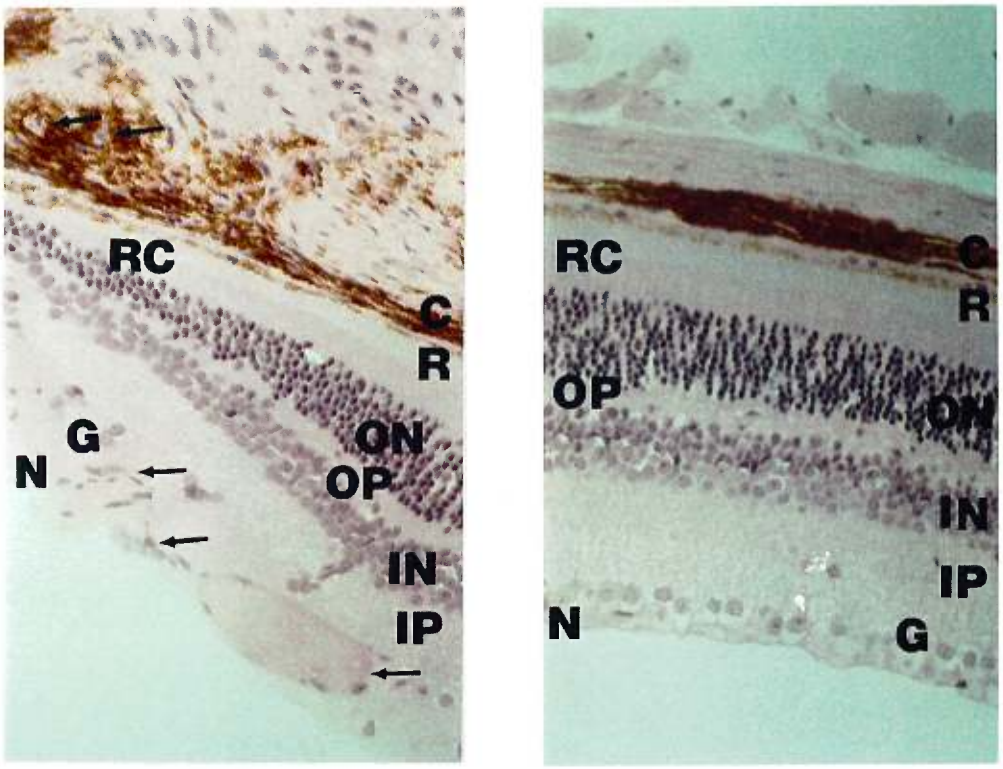

In the *stb/stb* picture eye abnormalities are indicated with arrows, in the choroid (C) we find vascularisation of the arteries and in the retina (R) we find perturbations of the nerve fiber (N) and ganglion (G) layers. Note the absence of such disturbances on the *stb/+* side. The inner plexiform (IP), inner nuclear (IN), outer plexiform (OP), outer nuclear (ON), rods and cones (RC) layers of the retina do not show any gross morphological differences. Pictures are 56.25X magnification.

B. The Cornea

stb/stb *stb/+*

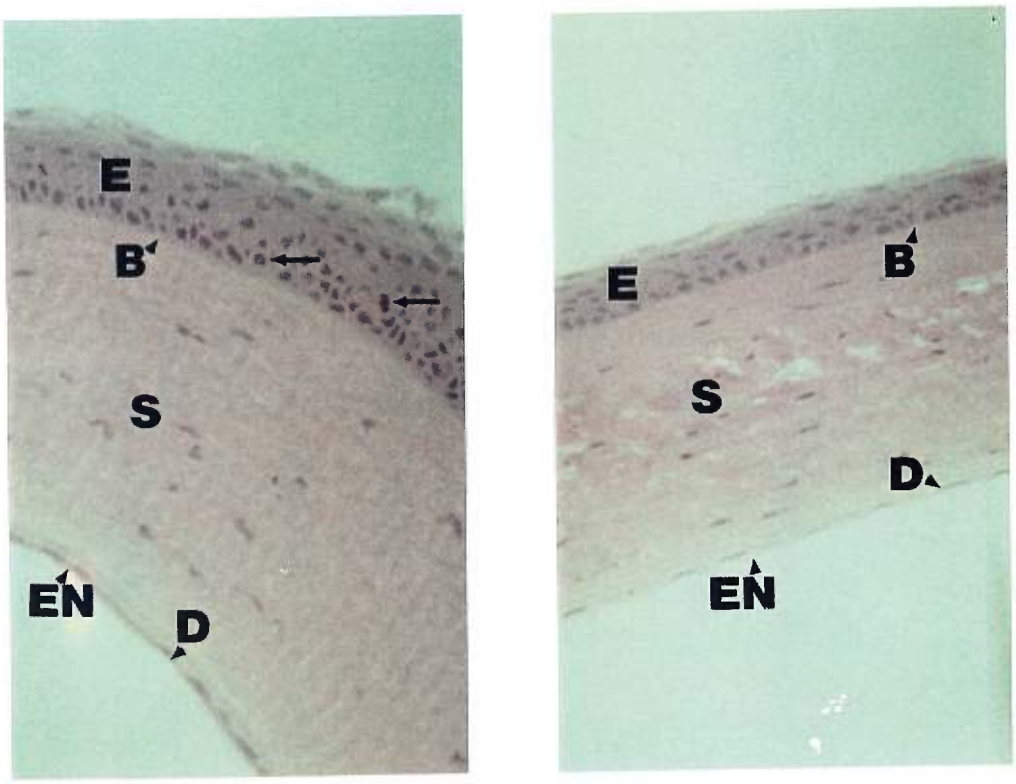

In the *stb/stb* picture we find extensive thickening (as compared to a normal littermate) of the corneal epithelium (E) with deposits indicated by arrow heads. Other layers of the cornea, such as; Bowman's membrane (B), stroma (S), Descemet's membrane (D) and endothelium (EN) appear the same. Pictures are 56.25X magnification.

Figure 7

RFLP analysis of restriction enzyme-digested gDNA of C57BL/6JEi and SPRET/Ei

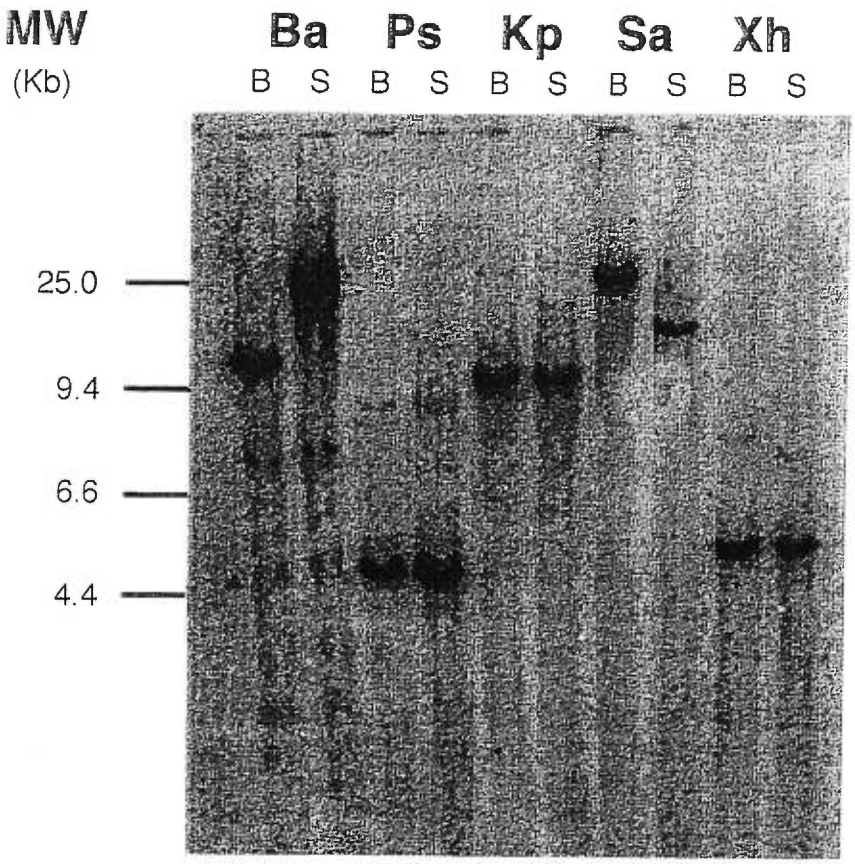

A *BamH* I (Ba) digestion of C57BL/6JEi (B) and SPRET/Ei (S) gDNA revealed an RFLP: 14.5 kb and 25 kb for B and S, respectively. Other restriction enzymes used are *Pst* I (Ps), *Kpn* I (Kp), *Sal* I (Sa) and *Xho* I (Xh). MW marks the molecular weight in kilobases (kb). A Sa RFLP was also observed between these two strains of mice.

BamH I-digested gDNA from 94 mice born of the backcross (C57BL/6JEi x SPRET/Ei) F1 x SPRET/Ei were analyzed by Southern blot to determine the proportion of homozygotes for the SPRET/Ei fragment and of heterozygotes carrying both SPRET/Ei and C57BL/6JEi fragments. A partial result is shown in Figure 8. Using the Map Manager program (Manly, 1993), the *Lhx3* recombination pattern was compared for identity to those pre-established at The Jackson Laboratory for many know loci using this backcross panel. This positioned the *Lhx3* gene on mouse Chr 2. The progeny haplotype derived from this analysis is shown in Figure 9. There were 0/94 recombination events between the *Lhx3* locus and the *Dbh* locus. Other loci that did not segregate from *Lhx3* include *Notch-1* and *Rxra1* (retinoid x receptor α). The *Dbh* locus was used as an anchor to integrate *Lhx3* in the consensus map of Lyon and Kirby (1994). In this consensus map, the *stb* mutation had been positioned close to *Dbh*.

The genetic mapping of *Lhx3* to mouse Chr 2 near the *stb* mutation and its preferential expression in the pituitary, a gland important for regulating growth and fertility, are the two major considerations that led us to embark into further molecular biological studies of *Lhx3* as a candidate gene for the *stb* mutation.

3.3. Search for RFLP of *Lhx3* Linked to the Stb Phenotype

The first step in this effort was to search for an RFLP of the *Lhx3* gene distinctive of the stubby phenotype. Such a RFLP could be an indication that mutations have indeed occurred in this gene and that may be the cause of the phenotype. It could be also a useful marker for genotyping offspring of mutant crosses. Thus, we performed a comparative Southern blot analysis of gDNA from *stb/stb* and *stb/+* mice using 12 restriction enzymes (*BamH* I, *Bgl* II, *EcoR* I, *EcoR* V, *Hind* III, *Kpn* I, *Msp* I, *Pst* I, *Sac* I, *Sal* I, *Xba* I and *Xho* I).

Figure 8

A partial BamHI-digested gDNA from individuals of the backcross panel

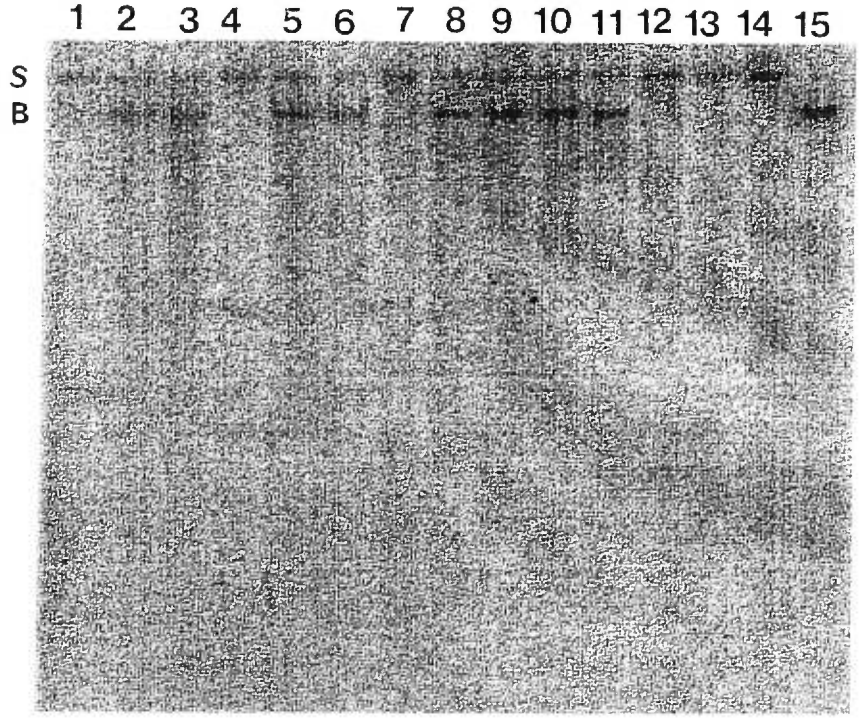

BamH I-digested gDNA from 15, out of 94, mice born of the backcross (C57BL/6JEi x SPRET/Ei) F1 x SPRET/Ei, are presented above. This Southern blot analysis determined the proportion of heterozygotes carrying both SPRET/Ei (S) and C57BL/6JEi (B) fragments of 25 kb and 14.5 kb, respectively and of homozygotes for the S fragment alone.

Figure 9

Progeny haplotype for mouse Chr 2

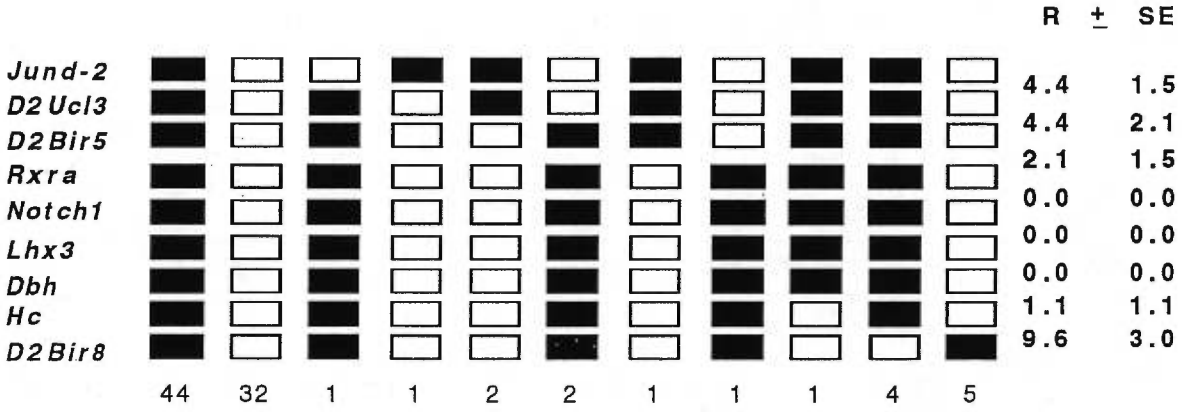

Loci are ordered vertically downward from the centromere. C57BL/6JEi and SPRET/Ei alleles inherited by the N2 progeny of the backcross are represented with black and white boxes, respectively. The number of offspring with each haplotype is indicated at the bottom of the corresponding column. The percent recombination (R) (± standard error, SE) for each pair of consecutive loci is indicated to the right.

Note that some of the enzymes were chosen because they contained CG dimers (*Bgl* II, *Msp* I, *Pst* I, *Sac* I) which are often methylated in eukaryotic cells and can undergo oxydative deamination leading to C to T transition. They are therefore mutation-prone sites.

As shown in Figure 10, no RFLP was observed with any of the enzymes tested. Furthermore, no gross abnormalities (deletions, insertions, inversion) of the *Lhx3* gene was detected in any of the *stb* mice. A more refined technique (as outlined below) was employed. The results do not exclude the possibility of point mutations not detectable with restriction enzymes.

3.4. SEQUENCING OF THE FUNCTIONAL DOMAINS OF THE *LHX3* GENE

We decided to apply a more refined technique involving sequencing of *Lhx3* exons to detect possible point mutations in *stb/stb* animals. The exon amplification and sequencing were performed by PCR (see section 2.9) on gDNA using exon-flanking primers derived from the cDNA sequence (see Figure 5). The primer sequences in the *Lhx3* cDNA, the annealing temperatures used during PCR and the size of their PCR products are shown in Table II.

We concentrated on the exons which encode the two LIM protein domains (LIM-A and LIM-B), the homeodomain (HD) and the 3'PEST region. The PCR sequencing was performed on gDNA of individual mice or on pools of gDNA from 8 *stb/stb* and 4 *stb/+* mice. The sequencing results are presented in Figure 11 for LIM-A and LIM-B domains; and in Figure 12 for part of the HD and PEST region.

We were intrigued by a difference that was consistently observed in both the LIM-A and the LiM-B domains of stb/stb relative to *stb/+* mice, on both pooled and on individual gDNA. They appeared as compression of the nucleotide bands in certain regions of the sequence. To exclude the possibility that this compression was due to a technical problem, we subcloned the PCR DNA corresponding to the LIM-A and LIM-B domains of 1 *stb/stb* and 1 *stb/+* mouse in the pCRII plasmid and expanded them in bacteria.

Figure 10

RFLP analysis of the Lhx3 gene

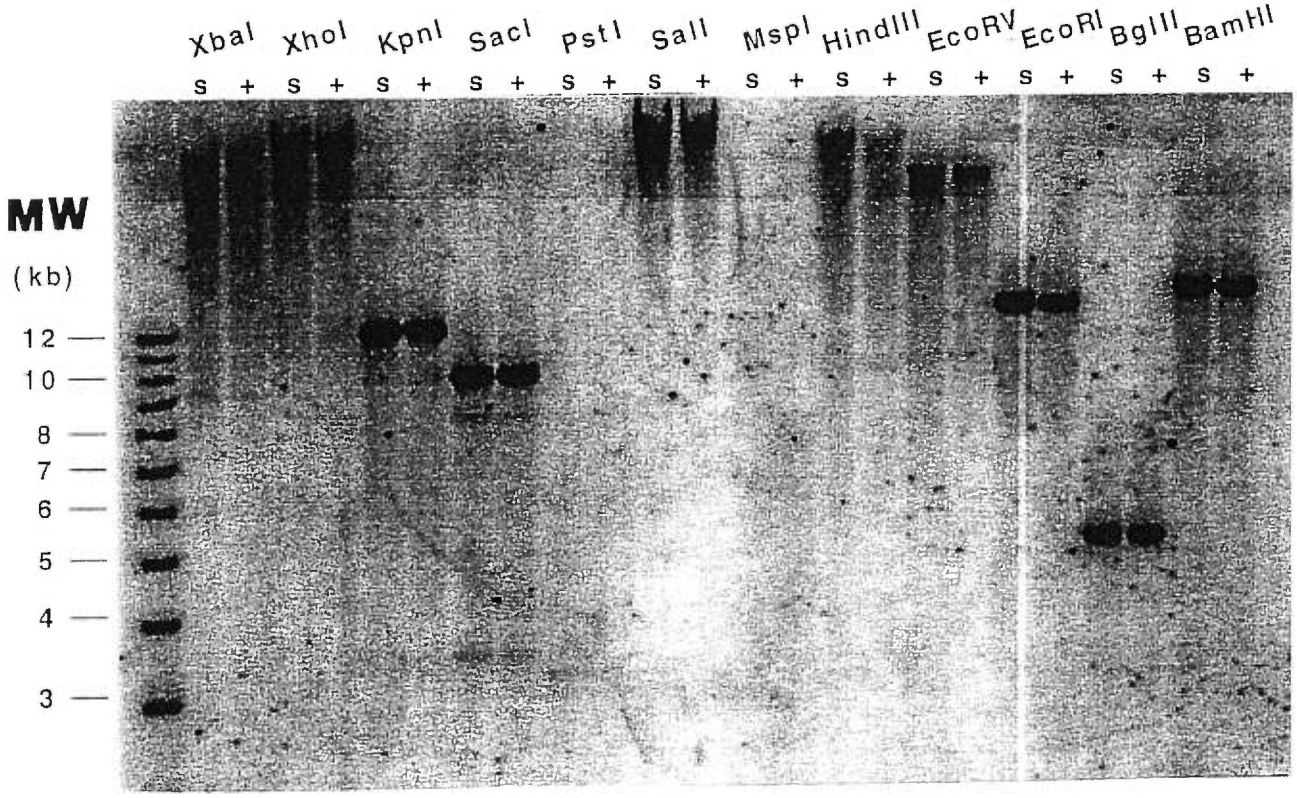

Of the 12 restriction enzymes used to digest gDNA from *stb/stb* (s) and *stb/+* (+) mice, no RFLP was observed. MW refers to the molecular weight of fragments in kilobases (kb).

TABLE II

Primers used for PCR sequencing of Lhx3 exons

PRIMERS	SEQUENCE	Ta (°C)	PRODUCT OF PCR (bp)
1S	GATCCCGATGTGTGCAG	52	166
1AS	AGAAGTCGTCTTTGCAG	52	-
2S	GCTTCGGGACCAAGTGC	52	198
2AS	GCTGCTTGGCTGTTTCG	52	-
3S	AGCCGAGGCCACAGCCA	58	149
3AS	GCACCACTCGCATGTCCA	58	-
P802	CCAGCCTGGTATACCCAGACAC	58	239
P807	GGCAGCACCAAGACCCCTGAG	58	-

Nucleotide sequences are presented from 5' to 3'; S and AS represent the sense and antisense primers used for amplification (refer to Figure 5 for positions). Ta corresponds to the PCR annealing temperature for each primer pair. The product of PCR is in base pairs (bp).

Figure 11

The sequence of LIM-A and LIM-B domains of the Lhx3 gene in stb/stb and stb/+ mice

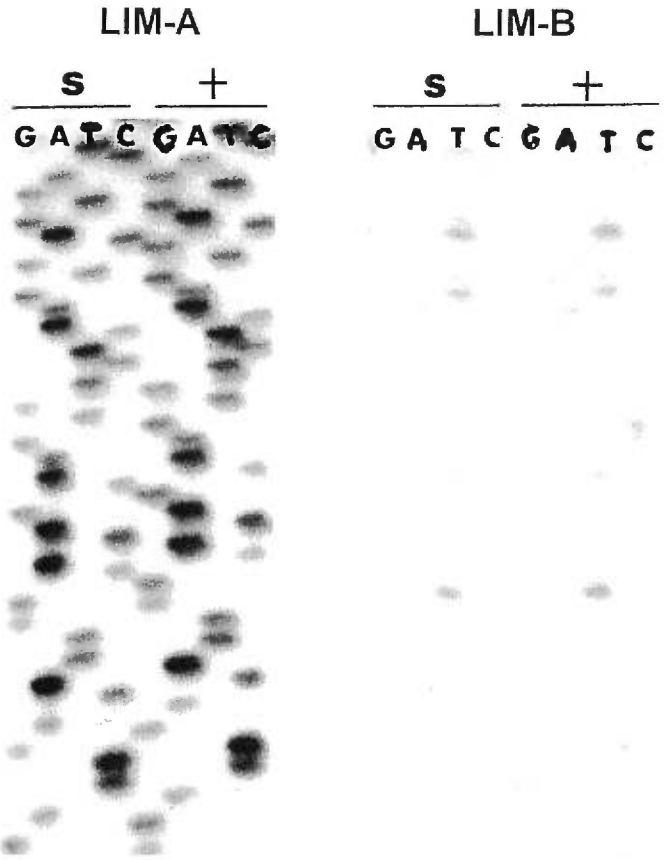

A partial nucleotide PCR sequence (G, A, T, C) of the LIM-A and LIM-B domains of *stb/stb* (s) and *stb/+* (+) mice is presented above. We found no differences between the two groups of mice.

Figure 12

The sequence of the homeodomain and PEST region of the Lhx3 gene in stb/stb and stb/+ mice

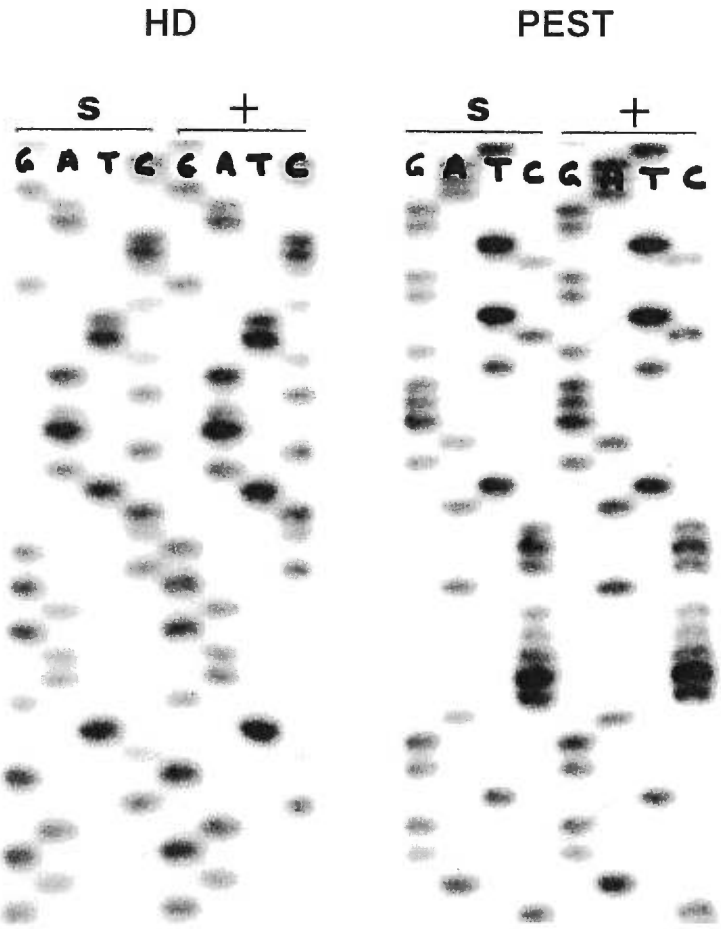

This figure presents a partial nucleotide PCR sequence (G, A, T, C) of the homeodomain (HD) and PEST region of *stb/stb* (s) and *stb/+* (+) mice. Again, no differences were found between the two groups of mice.

Sequencing of the subcloned fragments revealed no difference (results not shown), suggesting that that the difference initially observed was due to the PCR sequencing technique rather than to any kind of difference between *stb/stb* and *stb/+* mice.

Only the first half of the homeodomain encoded by exon 4, and the second half by exon 5 was sequenced. We encountered difficulties trying to amplify both exons 4 and 5, together. Again no differences in the sequence were identified between *stb/stb* and *stb/+* mice. Similarily, the PEST region, sequenced in its entirety, showed no differences between the two groups of animals.

It must be noted that not only was the second half of the homeodomain not sequenced, but intron-exon junctions were not looked at either. Therefore, possible differences may still exist between the *Lhx3* gene of *stb* and normal mice. Until the remaining sequences are determined, we can only conclude that out of the *Lhx3* cDNA bands amplified and sequenced, we did not find any differences between *stb/stb* and *stb/+* mice.

3.5. Northern Blot Analysis of Pituitaries

The structural analyses conducted in sections 3.3 and 3.4 having not yielded a difference, we asked whether there could be differences in the regulation of *Lhx3* and hormonal genes in the pituitary. As discussed in the introduction, this organ depends on the *Lhx3* gene product for its development and is the site of expression of hormones regulating growth and fertility. It is therefore possible that abnormal expression of *Lhx3* and its regulated genes could be associated with the stubby phenotype.

In a first experiment, the pituitaries of 8 +/+, 4 *stb/+* and 4 *stb/stb* animals were grouped (by genotype) and total RNA was extracted and analysed by Northern blot with radiolabeled cRNA probes for mlim3, rPRL, rGH and rPOMC.

As shown in Figure 13, Lhx3 mRNA levels were found to be similar whereas PRL, GH and POMC mRNA levels were slightly different among the three groups of mice. Relative to the mRNA levels observed in +/+ controls, GH levels were decreased in both the *stb/+* and *stb/stb* groups by 30% and 40%,

respectively. POMC levels were two times higher in the *stb/stb* group and were one and a half times higher in the *stb/+* group, than in the control group. PRL levels, on the other hand, were two times higher in the *stb/+* group and lower by 30% in the *stb/stb* group, relative to the control group.

These relative values were derived from a pool of pituitaries of mice of different ages and of both sexes; hence, displaying inconsistent hormonal conditions among different animals within the same group. We decided to analyze pituitary mRNA from 4 individual *stb/stb* and 4 individual *stb/+* male mice from the same litter. As Lhx3 mRNA level of expression in the pituitaries of the three groups of mice was found to be similar, it was not evaluated on individual mice. The results for rPRL, rGH, rPOMC, rTSH, rFSH and rLH are presented in Figure 14. When comparing average levels of mRNA within each genotype, we found a 60% increase in the level of FSH expression in the pituitaries of *stb/stb* mice relative to their normal littermates. The average transcript levels for the other 5 pituitary hormones were similar between the two groups (Table III). Interestingly, when each mouse was looked at individually, we found a trend of inverse correlation within the two groups for GH versus POMC and PRL versus FSH. For *stb/+* mice, the levels of POMC mRNA and GH mRNA are directly correlated whereas they were inversely correlated in *stb/stb* mice. In contrast, an inverse correlation was seen between the levels of FSH and PRL in *stb/+* mice whereas in *stb/stb* mice the level of the transcripts for these two hormones was directly correlated (Figure 15).

We have no ready explanation for these correlations. They may simply represent fluctuations due to the limited number of samples examined or to the semi-quantitative nature of our analytical method. In fact, the change in FSH levels between *stb/stb* and *stb/+* were the only ones found to be statistically significant.

Figure 13

A graphic representation of the levels of expression of Lhx3 and pituitary hormones in three groups of mice

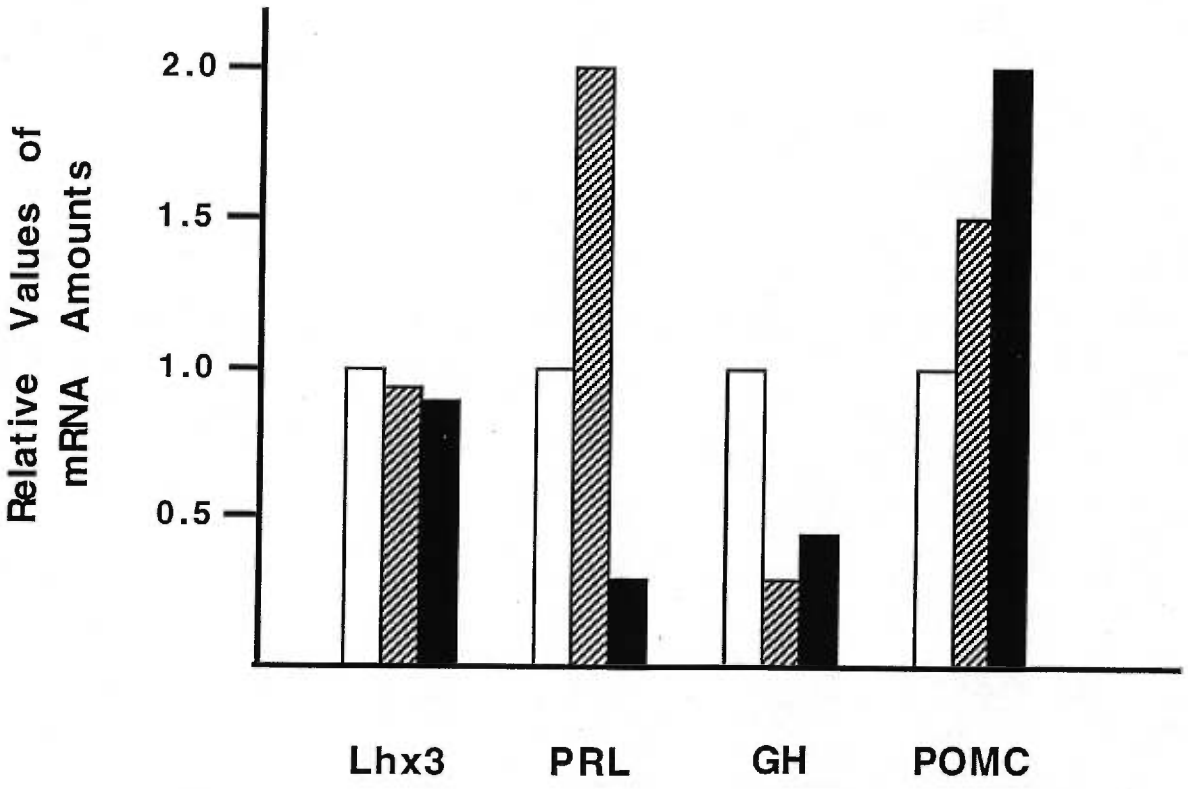

Values are represented after normalization for the amount of mRNA with the ribosomal 18S internal standard and take levels of expression of the +/+ group (clear bars) as a relative value of 1. The hatched bars and filled bars represent the *stb/+* and *stb/stb* groups, respectively.

Figure 14

Northern Blot analysis of the levels of expression of pituitary hormones in stb/stb versus stb/+ mice

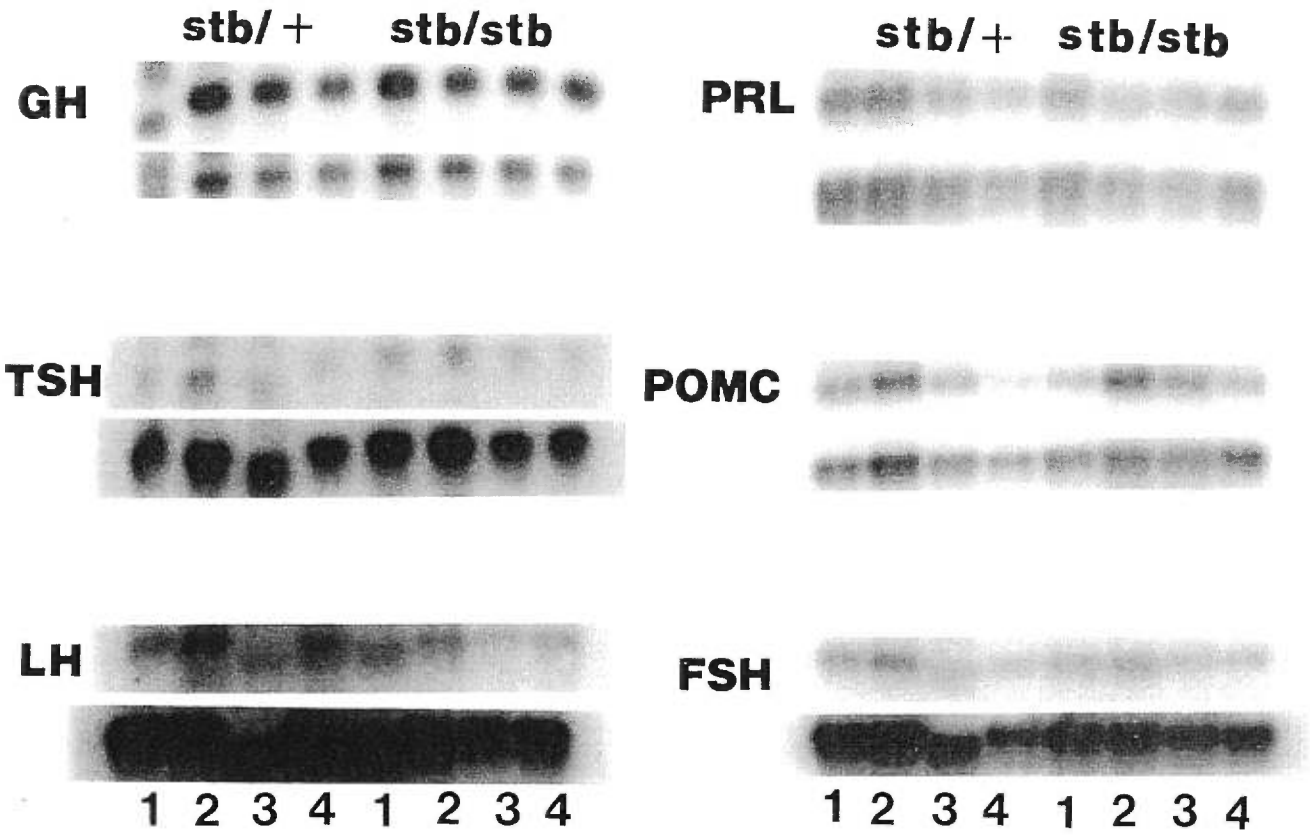

Messenger RNA from individual pituitaries of *stb/+* and *stb/stb* mice (numbered 1-4 under their corresponding phenotype) were analyzed by Northern blot. Six major pituitary hormones with their respective normalization of mRNA quantities, using the ribosomal 18S as internal standard, are listed at the left of each picture.

Table III

Relative values of the transcript levels of pituitary hormones expressed in stb/stb and stb/+ mice

	GH	POMC	PRL	FSH	TSH	LH
stb/stb						
1	3.29	0.52	1.09	0.37	0.17	0.47
2	2.43	1.32	1.05	0.32	0.16	0.53
3	0.97	0.97	1.20	0.53	0.23	0.55
4	3.91	0.52	1.33	0.54	0.21	0.69
X	**2.65**	**0.83**	**1.16**	**0.44**	**0.19**	**0.56**
SEM	0.95	0.31	0.10	0.10	0.03	0.07
σ	1.27	0.39	0.13	0.11	0.03	0.09
stb/+						
1	1.27	0.91	1.29	0.21	0.42	0.61
2	3.30	0.94	1.38	0.21	0.20	0.89
3	3.10	0.70	1.06	0.35	0.19	0.41
4	2.05	0.44	1.12	0.39	0.20	0.31
X	**2.43**	**0.74**	**1.21**	**0.29**	**0.25**	**0.55**
SEM	0.66	0.18	0.12	0.08	0.08	0.20
σ	0.01	0.23	0.15	0.09	0.11	0.26
t test	0.47	0.33	0.38	0.01*	0.21	0.49

Values represent the pixel count given for each band intensity after a phosphorimaging scan. The mean (X), standard error of mean (SEM) and standard deviation (σ) were calculated for each group of mice. The asteriks (*) highlights the statistical significance of FSH levels as calculated by the student t test.

Figure 15

Pituitary hormone transcript correlations found in stb/stb versus stb/+ mice

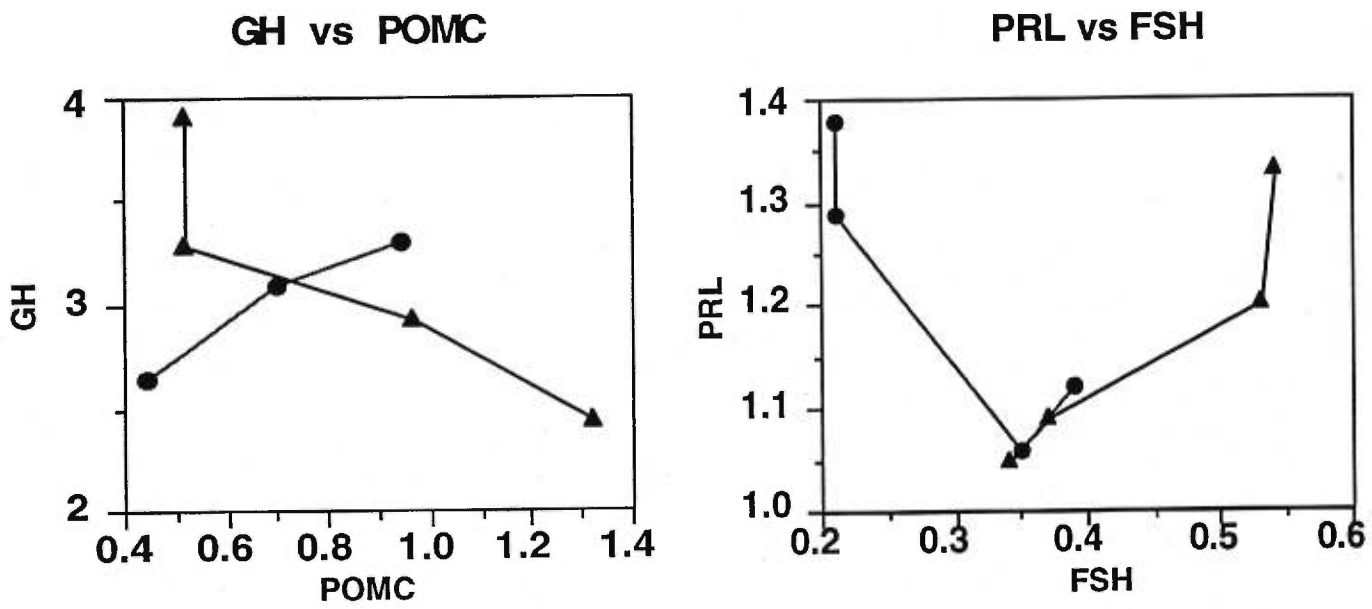

Hormonal transcript levels of individual mice as determined by Northern Blot analysis were shown to fluctuate significantly, yet correlations were found between *stb/+* and *stb/stb* groups of mice, for GH versus (vs) POMC and PRL vs FSH. The lines with arrows represent the *stb/stb* trend and the lines with circles represent the *stb/+* trend. Note the shift in the PRL vs FSH graph, identifying the increase in FSH transcript levels of *stb/stb* mice relative to their normal littermates.

3.6. Differential Display of Pituitary Gene Expression

The study, as conducted at this point, involved the structure or regulation of known target genes. Since no significant differences were observed, we wondered whether a global comparison of gene expression in *stb/stb* and *stb/+* pituitaries could provide new molecules that could be eventually investigated in relation with the stubby phenotype.

To this end, we used the differential display (DD) method, one of the most powerful analytical methods for gene expression. DD analysis of pituitary mRNA of individual *stb/stb* versus *stb/+* mice revealed reproducible differences in gene expression within these two groups (Figure 16). The differences in gene expression are outlined by the greater than symbol (representing those mRNAs which appear to be overexpressed) and asteriks (representing those mRNAs which appear to be underexpressed or silenced). These differing mRNAs may represent potential genes affected by the *stb* mutation.

Figure 16

Differential display analysis of pituitary mRNA from stb/stb and stb/+ mice

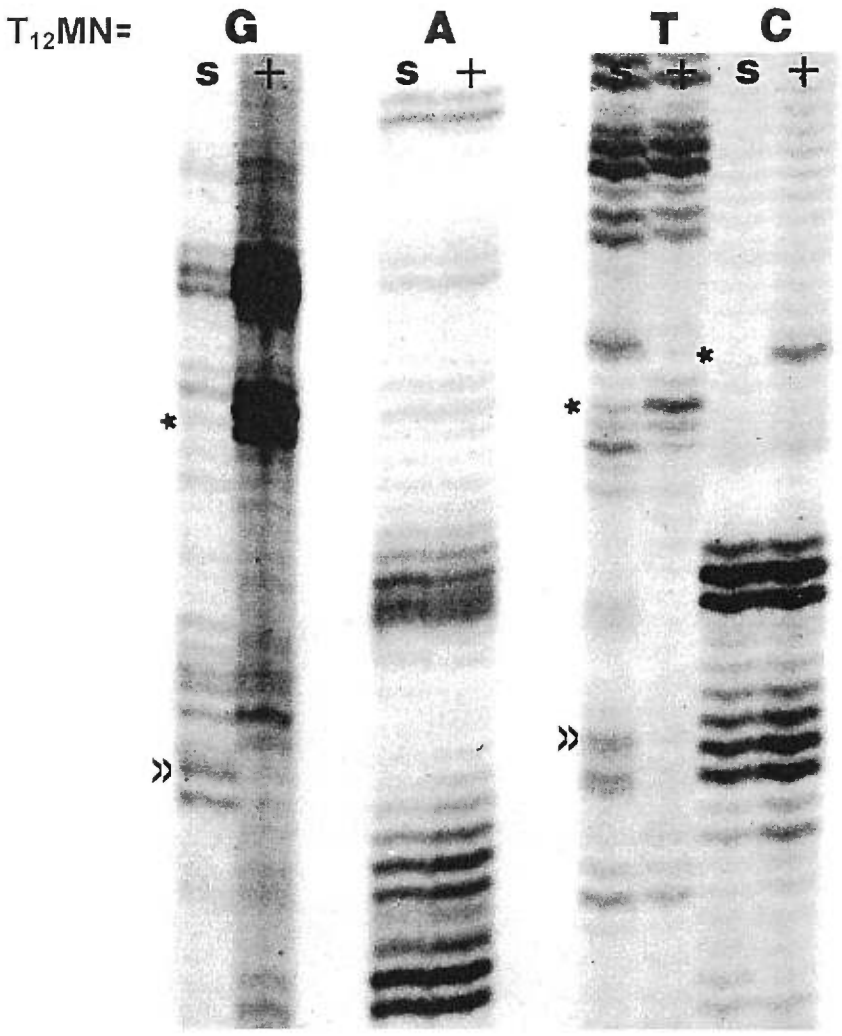

The $T_{12}MN$ (N = G, A, T, or C) used in the reaction is given on top of each column. Comparisons were made by migrating the *stb/stb* (s) samples along side the *stb/+* (+) samples. The asteriks (*) represents those differences which appear to be under expressed or silenced in the s samples, while the greater than symbol (») represents those differences which appear to be over expressed in the s samples.

4. DISCUSSION

The successful completion of a 5000 piece jigsaw puzzle is both an art form and a work of science. First comes the obvious question of finding those pieces of the puzzle which represent the sides (straight edged pieces), then one may begin to collect those pieces which share the same colours, motifs and are part of the same image in the picture. The most difficult and time consuming part would be in the fitting of the pieces together, by shape and shades of colours. More often than not your first guess is wrong but it eventually leads you to the right piece that fits. The puzzle in our case was investigating, by genetic and molecular biological means, a gene named *Lhx3*, as a candidate for the gene affected in a heritable phenotypic mutation called stubby.

The first indication of a possible association between *Lhx3* and *stb* came when we positioned it near the *stb* locus on Chr 2 in the consensus map of Lyon and Kirby (1994). The DNA backcross panel that provided the *Lhx3* allele distribution and segregation relative to other loci was derived from 94 N2 animals only and thus constitutes a moderate size panel. Larger panels can be analyzed to further tighten (or untighten) the linkage. Loci that did not segregate from *Lhx3* include *Notch-1* and *Dbh*. The *Jund-2* locus also maps close to the *Lhx3* locus but is located at approximately 4 cM (10^5 bp) away. All these loci, including *Lhx3*, represent potential genes for the *stb* mutation.

The mapping of a gene close to a known phenotypic mutation is not proof of its association with that mutation, but represents a starting point for further studies. The *stb* mutation causes growth abnormalities and impotence. Any candidate gene must be evaluated in relation to the possibility that its abnormal expression may cause the above phenotype. From the findings of Schlingensiepen et al. (1994), the Jund transcriptional factor is a negative regulator of cell growth in various cell lines. A member of the potent jun transcriptional factors, involved in neuronal differentiation, programmed neuronal cell death and neuronal plasticity, a *Jund2* mutation may have profound developmental consequences such as neurological defects. Its position on Chr 2

is distant from the *stb* locus, and therefore it is less likely to be linked to *stb.*

Notch-1, on the other hand is expressed early in mouse development in the developing central nervous system and during somitogenesis. It may play a role in proliferation and differentiation of the nervous system and peripheral tissues. This pattern of expression argues for the possibility that a mutation in the *Notch-1* gene could cause serious neurological abnormalities. As described in the introduction, erection in humans is to a certain extent neurogenic, and is initiated by visual, olfactory and tactile stimulation of the central nervous system. It has been found that any neurological disorder in humans which interrupts the nerve supply to the erectile tissues will generally cause an erectile failure (*www. Sexhealth.org/impotence.htm*). There is little known about the nerves which cause erection and therefore it is difficult to predict how damage to certain nerves will affect erectile capacity. This system has not been as detailed in the mouse. Whether *Jund2* or *Notch-1* are involved in the development of these neurological pathways remains to be determined.

The next candidate gene, *Dbh*, is expressed exclusively in noradrenergic and adrenergic cells and catalyzes the final step in noradrenaline synthesis (Stewart and Klinman, 1991). The recent inactivation of *Dbh* in mouse (Thomas and Palmiter, 1997) reveals that *Dbh*-null mice suffer from deficiencies of motor function, learning and memory; however, their fertility is normal, making *Dbh* an unlikely candidate for the *stb* mutation.

During the writing of this manuscript, we found an article which highlights the chromosomal mapping of mouse genes which are homologous to those found on human chromosome 9q. A gene for collagen proα1(V) chain (*Col5a1*), had previously been mapped to the distal human chromosome 9q and has now been assigned to mouse Chr 2 (Pilz et al., 1994) close to the *stb* mutation. One reason for *Col5a1*'s importance is that collagens constitute a large family of extracellular matrix components responsible for maintaining the structure and integrity of connective tissues such as those found in the penis. Type V collagen is a fiber forming collagen and is expressed in many connective tissues in man (Fessler and Fessler, 1997). The pattern of expression of *Col5a1* in mouse has

not been reported, yet the mapping position of *Col5a1* on the region of mouse Chr 2 and its implication in the eye problems of *stb/stb* mice, may suggest another possible candidate gene for the *stb* mutation.

4.1. Is Lhx3 Still a Candidate Gene for the Stb Mutation?

The focus of this report was to investigate the possible association of the *Lhx3* gene with the *stb* mutation. Our starting point was the positioning of the *Lhx3* locus in close proximity to that of *stb*. *Lhx3* gene expression in the pituitary, (primarily in the anterior and intermediate lobes) and more interestingly its vigorous expression in the hypophyseal primordium at e9.5 further strengthened our belief of its association with *stb*. The pituitary represents the primary organ responsible for growth and fertility and stubby mice are deficient in both. The expression of *Lhx3* in the central nervous system from e9.5 onward throughout the formation of the neural tube, hindbrain and spinal cord suggests that it may play an important function during these stages of development. This is further strengthened by the results found by Bach et al. (1997) where *Lhx3* was shown to be capable of transactivating pituitary-expressed promoters. The importance of *Lhx3* for the development of the pituitary is evident by the work of Sheng et al. (1996) who produced a mouse in which the gene was disrupted by homologous recombination. Their findings indicate that Rathke`s pouch (the hypophyseal primordium) was initially formed but failed to grow, yielding mutant embryos which lacked the anterior and intermediate lobes of the pituitary. This suggests that *Lhx3* is responsible for the cells of the pituitary primordium to commit to their specific lineages, but is not reponsible for the formation of the hypophyseal primordium itself. It must be noted that in this case it was a total disruption of the *Lhx3* gene. We may conclude that a total inactivation of the *Lhx3* gene does not produce the stb phenotype. What would happen in the case of a point mutation in this gene?

A novel symptom of the stubby phenotype was discovered in our colony of mice: *stb/stb* mice develop cataract-like defect in one or both eyes. The symptom appeared of particular relevance to us because of the expression of *Lhx3* in the

primordium of the pineal gland (Seidah et al., 1994). As soon as the lobular structures of the pineal gland become distinct at e16, *Lhx3* expression starts. Could *Lhx3* play a role in the proper development of this gland and if so, what possible consequences are there in the eye to a mutation in this gene?

Thus far, we are presented with a gene which is expressed in the pituitary, is vital for the normal development of this organ, functions as a transcriptional factor, is expressed in the development of the pineal gland and maps close to a phenotypic mutation where homozygous mice are deficient in growth, fertility and have eye problems. The next obvious step is to look by molecular biological means for any structural change caused by a mutation in the *Lhx3* gene as well as in its expression and of its potential regulation of other pituitary genes. A broad structural review of the *Lhx3* gene in *stb/stb* mice was performed by searching for RFLPs. Of the 12 restriction enzymes used, none gave a polymorphism between *stb/stb* mice and their *stb/+* littermates. The sequencing of each of the major domains of the *Lhx3* gene (LIM-A, LIM-B, HD and PEST) did not reveal any differences between *stb/stb* mice and their normal littermates, either. However, it must be recognized that the intron-exon junctions were not covered in this analysis and thus the possibility of a splicing mutation cannot be discounted. The coding region of *Lhx3* was not analysed completely and is therefore impossible to know if there are changes in the reading frame or the introduction of stop codons in a mutated gene. Moreover, the whole of the HD was not sequenced. As the HD in this transcriptional factor is a well established DNA-binding domain (Scott et al., 1989), a mutation in this region may cause impaired binding of the protein to its target genes. Ideally, the whole *Lhx3* gene, or at least its cDNA, should be sequenced in *stb/stb* mice and in their *stb/+* littermates to search for meaningful mutations. This long-term undertaking may be warranted if future evidence still points to *Lhx3* as the candidate gene for the *stb* mutation.

Next we concentrated on establishing the level of pituitary hormone mRNA in *stb/stb* mice versus their normal littermates, in hope of finding differences which may correlate with the capability of *Lhx3* as a transcriptional factor. The

pituitary hormones were chosen for the role they play in growth and fertility and of course their relative abundance in this organ. PRL was of particular interest as hyperprolactonemia in humans is a well established endocrine cause of impotence (Foster et al., 1990; Godeau and Charbonnel, 1993). We were unable to find any differences in the levels of PRL mRNA in these two groups of mice. Likewise GH, POMC, TSH and LH levels of expression were similar between *stb/stb* mice and their normal littermates. The only difference found within the two groups was the level of FSH transcription, which increased by 60% in the *stb/stb* mice. FSH secretion is negatively regulated by testicular inhibin. Whether the increase seen in the homozygous mutant mice is due to a inhibin deficiency is unclear. In any case, we have not found any reference of a possible link between FSH level and erectile dysfunction. A shortcoming of this analysis was the limited number of individual animals studied. Unfortunately, we experienced a regular shortage of animals, and this prevented us to thoroughly pursue this line of investigation. Obtaining *stb/stb* mice in our breeding colony was a serious limitation. As the *stb/stb* male mice are impotent, so the only possible way to generate *stb/stb* animals is to cross *stb/stb* females with proven *stb/+* males. These breedings were not efficient because litter sizes were usually quite small and many pups died before weaning. Purchasing the mice The Jackson Laboratory involved long delays of up to 3 months.

Finally, the novel technique of differential display was applied to the pituitaries of *stb/stb* mice versus their normal littermates to search for differences in gene expression, and excitingly, reproducible differences were observed. These differing mRNAs may represent additional leads towards the identification of the gene responsible for the *stb* mutation.

At this point it is hard to accept or dismiss the *Lhx3* gene as a candidate for the *stb* mutation. Further studies should be conducted for such a goal (as will be discussed in the next section). Overall, our work has tried to answer in a systematic fashion some of the most obvious questions of trying to associate (or dissociate) the *Lhx3* gene with the *stb* mutation. Even if we found no definite molecular differences in the *Lhx3* gene between *stb/stb* and *stb/+* mice, our

negative results have served to significantly narrow the scope of future investigations. Furthermore, with our discovery of the eye phenotype and differences in DD analysis, we think we have opened up new avenues of investigation for others to further pursue.

4.2. A Proposal for Future Work

Firstly, a Chr 2 polymorphic marker linked to *stb* should be found and linkage mapping performed with the *Lhx3* gene in a backcross mapping panel large enough to reduce the resolution to a fraction of a cM. The association of these two loci would be stronger if their segregation could not be achieved.

As mentioned above, the use of more *stb/stb* mice in studying the levels of pituitary hormones would greatly improve the statistical significance of our findings and perhaps discover other differences.

Lastly, and perhaps more importantly, the crossing of *stb/stb* females with heterozygous *Lhx3* mutant (*Lhx3+/-*) mice should reveal if this gene is responsible for the *stb* mutation. The genotypes of the offsprings of such a cross would be either *stb/Lhx3+* or *stb/Lhx3-*. If *Lhx3* is responsible for the *stb* mutation then one would expect that all those with the *stb/Lhx3-* genotype to exhibit the stubby phenotype.

5. CONCLUSION

Although not succesfully completed, some of the pieces of this puzzle (*Lhx3* and the stubby phenotype) are being assembled and have been matched together. The overall image that is before us is one of a stubby mouse, exhibiting disproportionate dwarfing; a fertility disorder represented by impotence; and eye problems in the form of cataracts and early corneal deposits (this being a novel addition to its phenotype). The gene mutation causing this phenotype has yet to be determined. Chomosomal localization of the *stb* locus has positioned it near candidate genes potentially responsible for this mutation, which include *Dbh*, *Notch-1*, *Jund-2*, *Col5a1* and *Lhx3*.

The inactivation of *Dbh* reveals that *Dbh*-null mice are deficient of motor function, memory and learning skills; however, their fertility is normal, making *Dbh* an unlikely candidate. *Notch-1* and *Jund-2* gene products, have been identified as important molecules in neuronal proliferation and differentiation. In humans, erectile function is to a certain extent neurogenic. These pathways have not been as detailed in the mouse, so the involvement of *Notch-1* and *Jund-2* in the erectile capacity in mouse remains to be determined. Although the pattern of expression of *Col5a1* in mouse has not yet been reported, it should be investigated further due to its association with collagenous tissues and its possible implication in penile erection. *Lhx3* has been the focus of this work and as yet, still remains the best candidate gene for the *stb* mutation.

Lhx3 was put on the list of potential candidate genes through its chromosomal localization near the *stb* locus on mouse Chr 2. This link was strengthened by its expression pattern, particularily in the pituitary, CNS and pineal gland; requirement for normal pituitary organogenesis and cell lineage differentiation; ability to transactivate pituitary genes, thereby regulating their expression in growth and development.

Our systematic attempt to locate a mutation in the *Lhx3* gene of *stb* mice has not succeeded, yet these attempts are not complete for the whole of *Lhx3* has not been covered. An overall study of the expression levels of major pituitary

hormones, (in hopes of finding differences which may correlate with the capability of *Lhx3* as a transcriptional factor) revealed an increase of FSH in *stb/stb* mice relative to their normal littermates. Unfortunately, we have not found any references of a possible link between FSH levels and erectile dysfunction. We also observed interesting hormonal correlations between GH versus POMC and PRL versus FSH in the two groups of mice. We have no ready explanation for these correlations, yet they may serve as trends to identifying the *stb* mutation.

A final, global comparison of gene expression in *stb/stb* and *stb/+* pituitaries through the technique of differential display, has revealed reproducible differences within these two groups. These differing mRNAs may represent additional leads towards the identification of the gene responsible for the *stb* mutation.

Overall, our work has tried to answer in a systematic fashion some of the most obvious questions in trying to associate the *Lhx3* gene to the *stb* mutation. Even if we found no definite molecular differences in the *Lhx3* gene between *stb/stb* and *stb/+* mice, our negative results have served to narrow the scope of future investigation, significantly. Furthermore, with our discovery of the eye phenotype and differences in the differential display analysis, we think we have opened up new avenues of investigation for others to further pursue.

6. BIBLIOGRAPHY

Archer, V. E., Breton, J., Sanchez-Garcia, I., Osada, H., Forster, A., Thomson, A. J., and Rabbitts, T. H. (1994). Cysteine-rich LIM domains of LIM-homeodomain and LIM-only proteins contain zinc but not iron. Proc. Natl. Acad. Sci. U.S.A. *91*, 316-20.

Ausubel, F. M., Brent, R., Kingston, R. E., Moore, D. D., Seidman, J. G., Smith, J. A., and Struhl, K. (1995). Current Protocols in Molecular Biology (New York, New York: Greene and Wiley).

Bach, I., Carriere, C., Ostendorff, H. P., Andersen, B., and Rosenfeld, M. G. (1997). A family of LIM domain-associated cofactors confer transcriptional synergism between LIM and Otx homeodomain proteins. Genes Dev. *11*, 1370-80.

Bach, I., Rhodes, S. J., Pearse, R. V. n., Heinzel, T., Gloss, B., Scully, K. M., Sawchenko, P. E., and Rosenfeld, M. G. (1995). P-Lim, a LIM homeodomain factor, is expressed during pituitary organ and cell commitment and synergizes with Pit-1. Proc. Natl. Acad. Sci. U.S.A. *92*, 2720-4.

Barnes, J. D., Crosby, J. L., Jones, C. M., Wright, C. V., and Hogan, B. L. (1994). Embryonic expression of Lim-1, the mouse homolog of Xenopus Xlim-1, suggests a role in lateral mesoderm differentiation and neurogenesis. Dev. Biol. *161*, 168-78.

Boehm, T., Foroni, L., Kaneko, Y., Perutz, M. F., and Rabbitts, T. H. (1991). The rhombotin family of cysteine-rich LIM-domain oncogenes: distinct members are involved in T-cell translocations to human chromosomes 11p15 and 11p13. Proc. Natl. Acad. Sci. U.S.A. *88*, 4367-71.

Bourgouin, C., Lundgren, S. E., and Thomas, J. B. (1992). Apterous is a Drosophila LIM domain gene required for the development of a subset of embryonic muscles. Neuron *9*, 549-61.

Chubb, C. (1987). Animal models of physiologic markers of male reproduction: genetically defined infertile mice. [Review]. Environ Health Perspect *74*, 15-29.

Chubb, C., and Nolan, C. (1985). Animal models of male infertility: mice bearing single-gene mutations that induce infertility. Endocrinology *117*, 338-46.

Cohen, B., McGuffin, M. E., Pfeifle, C., Segal, D., and Cohen, S. M. (1992). apterous, a gene required for imaginal disc development in Drosophila encodes a member of the LIM family of developmental regulatory proteins. Genes Dev. *6*, 715-29.

Crawford, A. W., Michelsen, J. W., and Beckerle, M. C. (1992). An interaction between zyxin and alpha-actinin. J. Cell Biol. *116*, 1381-93.

Dawid, I. B., Toyama, R., and Taira, M. (1995). LIM domain proteins. Comptes Rendus de l'AcadÈmie des Sciences - SÈrie III, Sciences de la Vie *318*, 295-306.

Fessler, J. H., and Fessler, L. I. (1997). Structure and Function of Collagen Genes, R. Mayne and R. E. Burgeson, eds. (Orlando: Academic Press).

Feuerstein, R., Wang, X., Song, D., Cooke, N. E., and Liebhaber, S. A. (1994). The LIM/double zinc-finger motif functions as a protein dimerization domain. Proc. Natl. Acad. Sci. U.S.A. *91*, 10655-9.

Fisch, P., Boehm, T., Lavenir, I., Larson, T., Arno, J., Forster, A., and Rabbitts, T. H. (1992). T-cell acute lymphoblastic lymphoma induced in transgenic mice by

the RBTN1 and RBTN2 LIM-domain genes. Oncogene 7, 2389-97.

Foster, R. S., Mulcahy, J. J., Callaghan, J. T., Crabtree, R., and Brashear, D. (1990). Role of serum prolactin determination in evaluation of impotent patient. Urology *36*, 499-501.

Freyd, G., Kim, S. K., and Horvitz, H. R. (1990). Novel cysteine-rich motif and homeodomain in the product of the Caenorhabditis elegans cell lineage gene lin-11. Nature *344*, 876-9.

German, M. S., Wang, J., Chadwick, R. B., and Rutter, W. J. (1992). Synergistic activation of the insulin gene by a LIM-homeo domain protein and a basic helix-loop-helix protein: building a functional insulin minienhancer complex. Genes Dev. *6*, 2165-76.

Godeau, T., and Charbonnel, B. (1993). Endocrinology of impotence. JournÈes Annuelles de Diabetologie de l'HÙtel-Dieu, 315-29.

Hermesz, E., Mackem, S., and Mahon, K. A. (1996). Rpx: a novel anterior-restricted homeobox gene progressively activated in the prechordal plate, anterior neural plate and Rathke's pouch of the mouse embryo. Development *122*, 41-52.

Karlsson, O., Thor, S., Norberg, T., Ohlsson, H., and Edlund, T. (1990). Insulin gene enhancer binding protein Isl-1 is a member of a novel class of proteins containing both a homeo- and a Cys-His domain. Nature *344*, 879-82.

Kosa, J. L., Michelsen, J. W., Louis, H. A., Olsen, J. I., Davis, D. R., Beckerle, M. C., and Winge, D. R. (1994). Common metal ion coordination in LIM domain proteins. Biochemistry *33*, 468-77.

Lane, P. W., and Dickie, M. M. (1968). Three recessive mutations producing disproportionate dwarfing in mice, achondroplasia, brachymorphic, and stubby. J. Hered. *59*, 300-308.

Lewin, B. (1990). *Genes IV.* Oxford University Press, New York, pp. 569-573.

Lyon, M. F., and Kirby, M. C. (1994). Mouse chromosome atlas. Mouse Genome *92*, 19-61.

Manly, K.F. (1993). A MacIntosh program for storage and analysis of experimental genetic mapping data. Mammal. Genome *4,* 303-315.

Maumenee, A. E. (1960). Congenital hereditary corneal dystrophy. *Am. J. Ophthal.* 50, 1114-1124.

McGuire, E. A., Rintoul, C. E., Sclar, G. M., and Korsmeyer, S. J. (1992). Thymic overexpression of Ttg-1 in transgenic mice results in T-cell acute lymphoblastic leukemia/lymphoma. Mol. Cell. Biol. *12*, 4186-96.

Michelsen, J. W., Schmeichel, K. L., Beckerle, M. C., and Winge, D. R. (1993). The LIM motif defines a specific zinc-binding protein domain. Proc. Natl. Acad. Sci. U.S.A. *90*, 4404-8.

Miller, W. A., and Flynn-Miller, K. L. (1976). A chondroplastic, brachymorphic and stubby chondrodystophies in mice. J. Comp. Pathol. *86*, 349-63.

Perez-Alvarado, G. C., Miles, C., Michelsen, J. W., Louis, H. A., Winge, D. R., Beckerle, M. C., and Summers, M. F. (1994). Structure of the carboxy-terminal LIM domain from the cysteine rich protein CRP. Nature Structural Biology *1*, 388-98.

Pilz, A., Prohaska, R., Peters, J., and Abbott, C. (1994). Genetic linkage analysis of the Ak1, Col5a1, Epb7.2, Fpgs, Grp78, Pbx3, and Notch1 genes in the region of mouse chromosome 2 homologous to human chromosome 9q. Genomics *21*, 104-9.

Rechsteiner, M. (1989). PEST regions, proteolysis and cell cycle progression. Revisiones Sobre Biologia Celular *20*, 235-53.

Roberson, M. S., Schoderbek, W. E., Tremml, G., and Maurer, R. A. (1994). Activation of the glycoprotein hormone alpha-subunit promoter by a LIM-homeodomain transcription factor. Mol. Cell. Biol. *14*, 2985-93.

Royer-Pokora, B., Loos, U., and Ludwig, W. D. (1991). TTG-2, a new gene encoding a cysteine-rich protein with the LIM motif, is overexpressed in acute T-cell leukaemia with the t(11;14)(p13;q11). Oncogene *6*, 1887-93.

Rugh, R. (1991). The mouse: Its Reproduction and Development (New York: Oxford University Press).

Sanchez-Garcia, I., Osada, H., Forster, A., and Rabbitts, T. H. (1993). The cysteine-rich LIM domains inhibit DNA binding by the associated homeodomain in Isl-1. EMBO J. *12*, 4243-50.

Schlingensiepen, K. H., Wollnik, F., Kunst, M., Schlingensiepen, R., Herdegen, T., and Brysch, W. (1994). The role of Jun transcription factor expression and phosphorylation in neuronal differentiation, neuronal cell death, and plastic adaptations in vivo. Cell. Mol. Neurobiol. *14*, 487-505.

Schmeichel, K. L., and Beckerle, M. C. (1994). The LIM domain is a modular protein-binding interface. Cell *79*, 211-9.

Scott, M. P. (1992). Vertebrate homeobox gene nomenclature. Cell *71*, 551-3.

Scott, M. P., Tamkun, J. W., and Hartzell, G. W. d. (1989). The structure and function of the homeodomain. Biochim. Biophys. Acta *989*, 25-48.

Seidah, N. G., Barale, J. C., Marcinkiewicz, M., Mattei, M. G., Day, R., and Chretien, M. (1994). The mouse homeoprotein mLIM-3 is expressed early in cells derived from the neuroepithelium and persists in adult pituitary. DNA Cell Biol. *13*, 1163-80.

Sheng, H. Z., Zhadanov, A. B., Mosinger, B., Jr., Fujii, T., Bertuzzi, S., Grinberg, A., Lee, E. J., Huang, S. P., Mahon, K. A., and Westphal, H. (1996). Specification of pituitary cell lineages by the LIM homeobox gene Lhx3. Science *272*, 1004-7.

Silver, L. M. (1995). *Mouse Genetics: concepts and applications.* Oxford University Press, New York, pp. 244-245.

Simmons, D. M., Voss, J. W., Ingraham, H. A., Holloway, J. M., Broide, R. S., Rosenfeld, M. G., and Swanson, L. W. (1990). Pituitary cell phenotypes involve cell-specific Pit-1 mRNA translation and synergistic interactions with other classes of transcription factors. Genes Dev. *4*, 695-711.

Stewart, L. C., and Klinman, J. P. (1991). Cooperativity in the dopamine beta-monooxygenase reaction. Evidence for ascorbate regulation of enzyme activity. J. Biol. Chem *266*, 11537-43.

Taira, M., Otani, H., Saint-Jeannet, J. P., and Dawid, I. B. (1994). Role of the LIM class homeodomain protein Xlim-1 in neural and muscle induction by the Spemann organizer in Xenopus. Nature *372*, 677-9.

Thomas, S. A., and Palmiter, R. D. (1997). Disruption of the dopamine beta-

hydroxylase gene in mice suggests roles for norepinephrine in motor function, learning, and memory. Behavioral Neuroscience *111*, 579-89.

Tsuchida, T., Ensini, M., Morton, S. B., Baldassare, M., Edlund, T., Jessell, T. M., and Pfaff, S. L. (1994). Topographic organization of embryonic motor neurons defined by expression of LIM homeobox genes. Cell *79*, 957-70.

Valge-Archer, V. E., Osada, H., Warren, A. J., Forster, A., Li, J., Baer, R., and Rabbitts, T. H. (1994). The LIM protein RBTN2 and the basic helix-loop-helix protein TAL1 are present in a complex in erythroid cells. Proc. Natl. Acad. Sci. U.S.A. *91*, 8617-21.

Way, J. C., and Chalfie, M. (1989). The mec-3 gene of Caenorhabditis elegans requires its own product for maintained expression and is expressed in three neuronal cell types. Genes Dev. *3*, 1823-33.

Williams, J.A., Paddock, S.W., Vorwerk, K., and Carroll, S.P. (1994). Organization of wing formation and induction of a wing patterning gene at the dorsal-ventral compartment boundary. Nature *368,* 299-305.

Wu, R. Y., and Gill, G. N. (1994). LIM domain recognition of a tyrosine-containing tight turn. J. Biol. Chem *269*, 25085-90.

Xue, D., Tu, Y., and Chalfie, M. (1993). Cooperative interactions between the Caenorhabditis elegans homeoproteins UNC-86 and MEC-3. Science *261*, 1324-8.

Zhadanov, A. B., Bertuzzi, S., Taira, M., Dawid, I. B., and Westphal, H. (1995a). Expression pattern of the murine LIM class homeobox gene Lhx3 in subsets of neural and neuroendocrine tissues. Developmental Dynamics *202*, 354-64.

Zhadanov, A. B., Copeland, N. G., Gilbert, D. J., Jenkins, N. A., and Westphal, H. (1995b). Genomic structure and chromosomal localization of the mouse LIM/homeobox gene Lhx3. Genomics *27*, 27-32.

APPENDIX

Article entitled:

Linkage mapping of the gene for LIM-homeoprotein LIM3 (locus *Lhx3*) to mouse Chromosome 2